

UNIVERSITA' DEGLI STUDI DI PARMA

Dottorato di ricerca in Scienze Chimiche

Ciclo XXVI (2011-2013)

**Evaluation of new active packaging
materials and analytical approaches**

Coordinatore:

Chiar.mo Prof. Roberto Cammi

Tutors:

Chiar.mo Prof. Claudio Corradini

Chiar.mo Prof. Angelo Montenero

Dottoranda: Claudia Lantano

Anno 2014

INDEX

Preface	8
CHAPTER 1: ANTIMICROBIAL ACTIVE COATING CONTAINING LYSOZYME FOR ACTIVE PACKAGING OBTAINED BY SOL-GEL TECHNIQUE	
1.1. Introduction	14
1.2. Materials and methods	20
<i>1.2.1. Chemical and Reagents</i>	20
<i>1.2.2. Sol synthesis and deposition</i>	21
<i>1.2.3. Fourier-transform infrared spectroscopy assay</i>	22
<i>1.2.4. Morphological characterization of films</i>	22
<i>1.2.5. Antimicrobial activity by agarose lysoplate method</i>	23
<i>1.2.6. HPLC lysozyme assay</i>	23
<i>1.2.7. Measure of antimicrobial activity of coatings by turbidimetric lysozyme assay</i>	26
1.3. Results and discussion	27
<i>1.3.1. ATR–FTIR spectra</i>	28
<i>1.3.2. Morphology of the films by AFM</i>	31
<i>1.3.3. In vitro antimicrobial activity of modified packaging</i>	32
<i>1.3.4. Kinetic release of lysozyme from coating to a liquid medium</i>	35
<i>1.3.5. Evaluation of antimicrobial activity of lysozyme released from films</i>	38
1.4. Conclusions	40
1.5. References	41

CHAPTER 2: NATAMYCIN BASED SOL-GEL ANTIMICROBIAL COATINGS ON POLYLACTIC ACID FILMS FOR FOOD PACKAGING

2.1. Introduction.....	50
2.2. Materials and methods.....	52
2.2.1. <i>Materials.....</i>	<i>52</i>
2.2.2. <i>Coatings preparation.....</i>	<i>53</i>
2.2.3. <i>Fourier-transform infrared spectroscopy.....</i>	<i>54</i>
2.2.4. <i>Activity evaluation of natamycin coatings in contact with cheese sample.....</i>	<i>55</i>
2.2.5 <i>Release of natamycin from coated films to food simulant</i>	<i>55</i>
2.3. Results and discussion.....	56
2.3.1. <i>Chemical and physical characterization of the films.....</i>	<i>56</i>
2.3.2. <i>ATR-FTIR spectra.....</i>	<i>58</i>
2.3.3. <i>Tests of mould growth on cheese samples.....</i>	<i>61</i>
2.3.4. <i>Release of natamycin from films.....</i>	<i>62</i>
2.4. Conclusions.....	67
2.5. References.....	68

CHAPTER 3: EFFECTS OF INNOVATIVE/ALTERNATIVE STEEPING METHODS ON ANTIOXIDANT CAPACITY, CAFFEINE ,CATHECHINS AND GALLIC ACID CONTENT OF GREEN, BLACK AND OOLONG TEA INFUSIONS

3.1. Introduction.....	76
3.2. Materials and methods.....	78
3.2.1. <i>Reagents and chemicals.....</i>	78
3.2.2. <i>Teas and preparation of infusions.....</i>	79
3.2.3. <i>High-performance liquid chromatography (HPLC) ...</i>	80
3.2.4. <i>Total phenolic content (TPC)</i>	82
3.2.5. <i>Determination of ferric reducing antioxidant power (FRAP).....</i>	82
3.2.6. <i>Statistical analysi.....</i>	83
3.3. Results and discussion.....	83
3.3.1 <i>High-performance liquid chromatography (HPLC).....</i>	83
3.3.2 <i>Total phenolic content</i>	89
3.3.3. <i>FRAP value.....</i>	91
3.4. Conclusions.....	92
3.5. References.....	93

CHAPTER 4: DEVELOPMENT OF NEW A ANALYTICAL METHODS FOR THE DETERMINATION OF POTENTIALLY TOXIC SUBSTANCES RELEASED FROM POLYCARBONATE IN CONTACT WITH FOOD

4.1. Introduction.....	100
4.1.1. <i>Polycarbonate.....</i>	<i>100</i>
4.2. Materials and method	103
4.2.1. <i>Chemicals, Reagents and Materials.....</i>	<i>103</i>
4.2.2. <i>Sample treatment.....</i>	<i>104</i>
4.2.3. <i>Analysis of the PC composition by GC-FID-IR.....</i>	<i>105</i>
4.2.4. <i>FT-IR ATR spectroscopy.....</i>	<i>106</i>
4.3. Results and discussion.....	107
4.3.1. <i>GC-FID-IR analysis.....</i>	<i>107</i>
4.3.2. <i>FT-IR analysis in ATR mode.....</i>	<i>113</i>
4.3.2.1. <i>Photo-aging of PC.....</i>	<i>113</i>
4.3.2.2. <i>Study of residues of detergent and sparkling aid.....</i>	<i>114</i>
4.4. Conclusions.....	116
4.5. References.....	116
SUMMARY.....	120

Preface

Food packaging is the largest consumer packaging segment, representing more than half of the total packaging market. The basic functions of packaging are to protect from physical atmospheric and human environments, to provide required information to consumers and to make food convenient in handling and transport during distribution and marketing.

More recently, new packaging materials known as “active packaging” have been developed increasing the functionality of the traditional package: food, package and the environment between them interact in a synergistic way to obtain a desired outcome. Antimicrobial packaging is a form of active packaging in which antimicrobial agents can be incorporated inside polymers or coated and adsorbed onto polymer films with the aim to extend the shelf life maintaining the quality of the food product.

Despite the benefits of packaging, many negative implications can be detrimental to quality and/or safety of food due to the tendency of some chemical substances to migrate from packaging to food content. Among other materials, plastics have emerged for primary food packaging: polycarbonate (PC), polyvinylchloride (PVC), high and low density polyethylene (HDPE and LDPE), polypropylene (PP), polyethylene terephthalate (PET) polystyrene (PS) are commonly used in the food packaging industry. Some of these materials, such as polycarbonate, may contain additives and other low molecular weight compounds (plasticizers, antioxidants, anti-UV, etc.) in order to improve their chemical and physical properties.

The present Ph.D thesis deals with the development of new active packaging and with the study of several aspects of “food contact materials”, organized into four chapters.

In Chapter 1 a new antimicrobial active packaging based on a sol–gel modified poly(ethylene terephthalate) (PET) is presented. Lysozyme is used as antimicrobial agent and incorporated into a hybrid organic-inorganic coating in order to achieve a controlled release. FTIR microspectroscopic and tapping mode-Atomic Force Microscopy (TM-AFM) measurements are used to characterize the prepared coatings. The antimicrobial activity of the obtained surface modified films was tested on agar plates against *Micrococcus lysodeikticus*. Furthermore, the stability of the coating was evaluated in order to verify a possible migration of lysozyme to a liquid media due to a possible release from the plastic substrate. The quantitative determination of the released active substances in the buffered solution was performed by HPLC UV-DAD.

Chapter 2 deals with a comprehensive study of a hybrid organic-inorganic coating with antimycotic properties. An active packaging based on polylactic acid was realized by sol-gel processing, employing tetraethoxysilane as a precursor of the inorganic phase and polyvinyl alcohol as organic component. Natamycin was incorporated as an active agent. Films with different organic-inorganic ratio were prepared, and the amount of antimycotic entrapped is found to be possibly modulated by the sol composition. FTIR microspectroscopic measurements are used to characterize the prepared coatings. The antifungal properties of the films were investigated against moulds growth on the surface of commercial semi-soft cheese. The release of natamycin from the films to ethanol 50% (v/v) was studied by HPLC

UV-DAD and the amount of antimycotic released to food simulating liquid is below the value allowed by legislation.

In Chapter 3 the effects of alternative steeping methods on tea infuses obtained from green, black and oolong teas were presented, in order to evaluate the best extraction conditions of antioxidants to be used in active packaging. The most important classes of compounds contained in the tea preparations, such catechins, xanthines and gallic acid were analysed by HPLC-DAD. Antioxidant assay and evaluation of total phenolic content were also performed.

Finally, in Chapter 4 the development of a new analytical method for the determination of potentially toxic substances released from commercial polycarbonate tableware in contact with food was reported.

To evaluate the composition of these substances, total dissolution of polycarbonate with chloroform and polymer reprecipitation with methanol have been used. The extract, containing monomers, oligomers, degradation products and other additives has been analyzed by GC coupled with flame-ionization detector (FID) with Fourier Transform Infrared Spectroscopy.

To evaluate the polymer photo-ageing, experiments in a climatic chamber on samples stored at room temperature and light exposure were investigated. The possible variations of the macromolecular structure of the polycarbonate were analyzed by FT-IR in ATR mode.

Finally the effects of treatment with detergents and sparkling solution on polycarbonate samples were studied by FT-IR in ATR mode.

Claudia Lantano

Chapter 1

Based on:

Antimicrobial active coating containing lysozyme deposited on PET obtained by sol–gel technique

By:

Corradini, C., Alfieri, I., Cavazza, A., Lantano, C., Lorenzi, A., Zucchetto, N., Montenero, A.

Published in *Journal of Food Engineering*, 119, 580–587 (2013).

1.1. Introduction

In recent years, controlled release systems have been used in food packaging thus becoming part of a wide category of new materials known as “antimicrobial active packaging”, which are one of the most promising alternatives to traditional packaging (Coma, 2008).

Promising active packaging systems include oxygen, and ethylene scavenging (Anthierens et al., 2011), CO₂-scavengers and emitters (McMillin, 2008), moisture regulators, release or adsorption of flavours and odours (Appendini and Hotchkiss, 2002), as well as the incorporation of antioxidants (Hauser and Wunderlich, 2011) to reduce oxidation of the food.

Several compounds have been successfully incorporated into packaging materials to confer antimicrobial activity such as organic acids (Muriel-Galet et al., 2012; Hauser and Wunderlich, 2011), inorganic nanoparticles (de Azeredo, 2013), essential oils (Manso et al., 2013; Seydim and Sarikus, 2006) various plant extracts (Wang et al., 2012), bacteriocins (Hanušová et al., 2010) and enzymes (Sunga et al., 2013).

Lysozyme (1,4-beta-N-acetylmuramidase, 14.4 KDa), is a hydrophilic protein that has been well characterized and widely used as a natural biopreservative for packaging applications (Proctor and Cunningham, 1988). It is abundant in a number of secretions, such as tears, saliva, human milk, and mucus, and large amounts can be found in egg white. It is a hydrolytic, secreted enzyme of 129 amino acids (Fig. 1), which folds into a compact globular structure; it plays an important role in preventing bacterial infection, especially for Gram-positive bacteria, due to the fact that their membrane is made up of 90% peptidoglycan

Antimicrobial packaging applications employing lysozyme have been studied by several authors (Barbiroli et al., 2012; Gemili et al., 2009; de Souza et al., 2009; Buonocore et al., 2005) and the diffusion of antimicrobial compounds from packaging materials has been widely reviewed by (Suppakul et al., 2003; Han, 2000; Buonacore et al., 2003). Recently, antimicrobial packaging materials have been obtained by the incorporation of lysozyme into polyvinyl alcohol (Conte et al., 2007; Mastromatteo et al., 2011), cellulose-based films (Gemili et al., 2009) and zein based films (Mecitoglu et al., 2006; Gucbilmez et al., 2007).

The present work was aimed at obtaining and characterizing a new food packaging by sol-gel methodology through incorporating lysozyme as an antimicrobial agent. The sol-gel process may be described as: "formation of an oxide network through polycondensation reactions of a molecular precursor in a liquid". This process can be employed for the preparation of glasses and ceramics, and also applied to the synthesis of hybrid organic-inorganic networks with controlled composition (Minelli et al., 2010).

In this work, active coatings were realized with the sol-gel methodology employing polyvinyl alcohol (PVOH, Fig. 3) as organic component and tetraethoxysilane (TEOS, Fig 3) as a precursor of the inorganic phase. The mentioned polymer is frequently used as a matrix for the immobilization of various enzymes and cells because of its easy availability, low price and FDA approval (Buonocore et al., 2003).

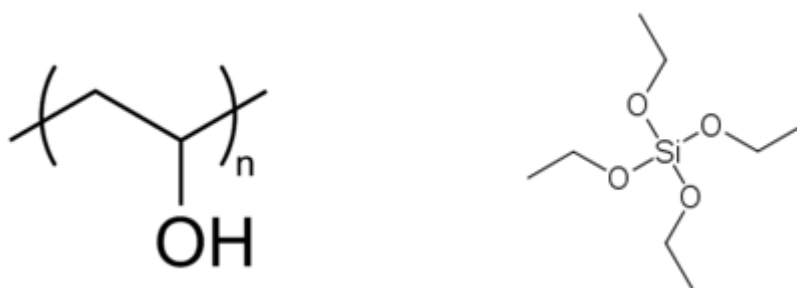


Fig. 3. Chemical structure of PVOH (left) and TEOS (right)

The sol-gel coating process consists of two distinct reactions: hydrolysis of the alcohol groups and condensation of the resulting hydroxyl groups. The first reaction occurs by the nucleophilic attack of the oxygen contained in water on the silicon atom with significant S_N2-type character (Fig. 4).

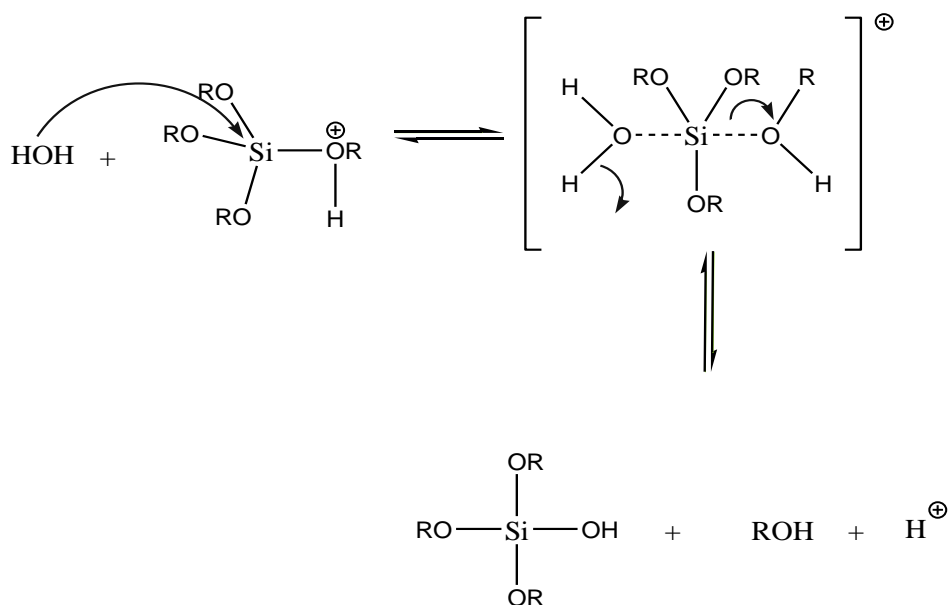


Fig. 4. Hydrolysis mechanism in acid catalyzed conditions

The silanol groups, formed in the hydrolysis process, tend to polymerize with formation of bonds Si - O - Si (Fig.5). Possible mechanisms are two: attack with elimination of a molecule of alcohol in the case of a partially hydrolyzed monomer (dealcoholation) or attack a silanol group on a silicon atom with subsequent expulsion of a molecule of water dehydration.

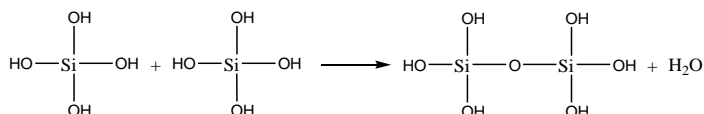


Fig. 5. Condensation

The condensation reaction with other groups \equiv Si-OH leads to a polycondensation reaction (fig.6), the water and the alcohol expelled remain in the pores of the network.

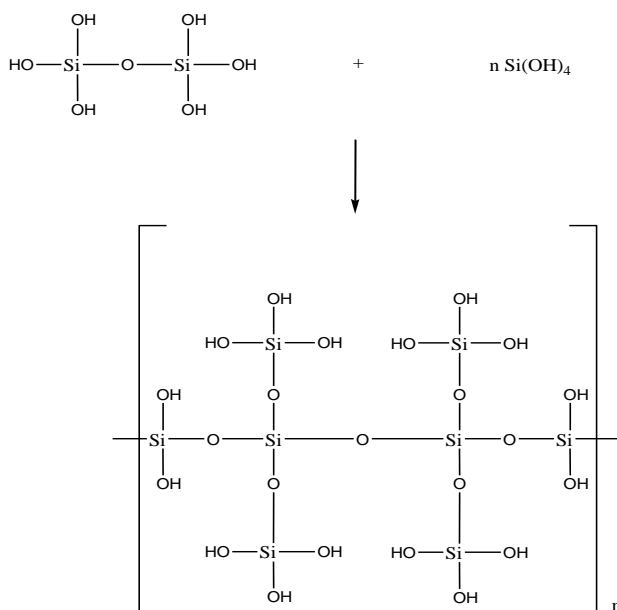


Fig. 6. Polycondensation

The most important advantages of this technique are the simple reactions involved, the low temperature of operation and the easy deposition onto polymeric substrates by dip, spin, or roll coating (Minelli et al., 2010). In the present work the coatings were deposited on poly(ethylene terephthalate) (PET) substrates by dip coating (Fig. 6). PET is a thermoplastic polymer which has found increasing applications as a food packaging material. PET is formed from the intermediates, terephthalic acid and ethylene glycol, which are both derived from oil feedstock. Dip coating is simple technique which consists of the immersion and withdrawal vertically of a substrate from a fluid sol at constant speed (Fig.7). The substrate is left to dry and then treated at the desired temperature. The film thickness is a function of the speed of extraction, the viscosity of the solution and of its nature.

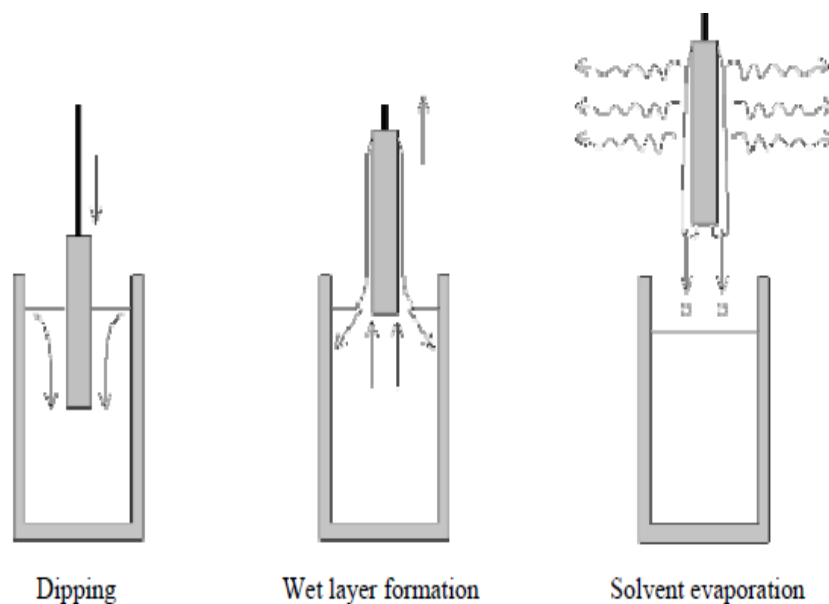


Fig. 7. Schematic phases of the dip coating process

PET was treated with cold plasma before deposition to improve adhesion propriety. Trough this technique the plasma is generated by subjecting low-pressure gas/ses in a vacuum chamber to an high frequency electromagnetic field, triggering a visible light discharge. In this way, an highly reactive process gas, which reacts on the surface of the product to be treated, is generated. For every process suitable parameters must be found, modifying the power, the frequency, the gas flow and ratios and the process time.

The preparation of organic–inorganic hybrid coatings by a sol–gel process presents several advantages such as high purity of the reactants and of the resulting products, mild processing conditions (low temperature, atmospheric pressure), possibility of controlling connectivity and morphology (Marini et al., 2007).

The antimicrobial activity, and the stability of the resulting material were tested.

The proposed technique allows to use a little amount of active substance, does not require a modification of the plastic production processes and it is easy to be realized.

1.2. Materials and methods

1.2.1. Chemical and reagents

Polyvinyl alcohol (PVOH) (MW = 88,000–97,000) was purchased from Alfa Aesar (Karlsruhe, Germany), tetraethoxysilane (TEOS) was supplied by Sigma–Aldrich (Gallarate, Italy). Reagent grade hydrochloric acid (37%, v/v) and all the other chemicals of analytical grade were obtained from J.T. Baker (Denver, Holland). The active compound was lysozyme from hen egg white (Sigma–Aldrich,

Gallarate, Italy). Trifluoroacetic acid (spectrophotometric grade), acetonitrile (HPLC grade) and *M. lysodeikticus* were purchased from Sigma–Aldrich Co. (UK). Deionized water (18 MX cm resistivity) was obtained from a Milli-Q Element water purification system (Millipore, Bedford, USA). All other reagents were analytical grade and were purchased from Sigma and Aldrich Co., unless stated otherwise.

1.2.2. Sol synthesis and deposition

The active coatings were obtained by a modification of a sol–gel method previously reported (Minelli et al., 2010). Briefly, at the first step 0.75 g of PVOH were dissolved into 40 mL of distilled water at 84 °C for 2 h and mixed under continuous magnetic stirring in a tightly closed bottle to prevent evaporation. The obtained homogeneous solution was slowly cooled at room temperature and was mixed with an appropriate amount of TEOS and immediately after with 27 µL of a 37% aqueous solution of HCl. Then, the sol was stirred at room temperature before adding 50 mg of lysozyme. An amount of sol without lysozyme was also prepared for negative controls. The films were obtained by dip-coating process. A homemade system was used for the dip-coating process, employing substrates with size 25 x 50 mm² and operating vertically at a constant speed of 7.0 cm/min. PET substrates were previously activated by cold plasma using a “Colibri” device manufactured by Gambetti Vacuum SrL (Binasco, Mi, IT) operating in air for 30 s at 54 W, within the absolute pressure range of 0.1–1 mbar. After deposition, the obtained coated PET films were dried in oven at 40°C (±1°C) for 10 min.

1.2.3. Fourier-transform infrared spectroscopy assay

The attenuated total reflection (ATR) method is based on the measurement of an infrared beam after it is reflected by the sample. An incident IR beam is directed onto an optically dense crystal with a high refractive index at a certain angle. This internal reflectance creates an evanescent wave that extends beyond the surface of the crystal into the sample held in contact with the crystal. In regions of the infrared spectrum where the sample absorbs energy, the evanescent wave will be attenuated. The detector records the attenuated IR beam as an interferogram signal, which can then be used to generate an infrared spectrum. ATR is indicated for the study of strongly absorbing or thick samples, as well as the surface layer of a multi-layered material or the coating on a solid.

FT-IR microspectroscopic measurements were performed using a Nicolet Nexus spectrometer by using a Pike Smart MIRacle™ single reflection horizontal attenuated total reflection (HATR) accessory equipped with a flat, polished zinc selenide crystal of 2 mm (all from Thermo Fisher, Germany). Spectra were collected in the spectral range from 4000 to 500 cm^{-1} on samples directly put in contact with the crystal, without any treatment.

1.2.4. Morphological characterization of films

In order to gather information about the surface and morphology of the obtained coating, tapping mode-Atomic Force Microscopy (TM-AFM) measurements were carried out using a PARK XE-100 atomic force microscope (AFM, Park System Corp., Suwon, Korea) at room temperature with silicon nitride cantilever (Olympus, Japan), which

has a resonant frequency of 265 kHz and a spring constant about 25.5 N/m. 10 µm x 10 µm pictures were acquired, root mean squared roughness (Rq) calculated for each surface and then averaged among 3 independent investigations. The following samples were analyzed: not treated PET (TQ) and coated PET prior and after an immersion test (La storia et al., 2008).

1.2.5. Antimicrobial activity by agarose lysoplate method

Lysozyme activity was tested according to a modified version of the Lie et al. method (Lie et al., 1986). A 1% agarose gel plate in 50 mM phosphate buffer (pH 6.2) containing 1 mg/mL of *Micrococcus lysodeikticus* (Sigma) was prepared and poured in Petri plates (45 mm in diameter) (Minagawa et al., 2001). After solidification, squared plates of coated films (1 x 1 cm²) containing lysozyme, as well as negative controls (untreated film samples), were laid on the gel. Plates were then incubated either at room temperature (RT) and at 37°C for 24, 48 and 182 h, and lysozyme activity was assessed as a clear zone of lysis around the plastic material. Quantitative evaluation of the antimicrobial activity was assessed by measuring the diameter of the cell walls lysis area around the films.

1.2.6. HPLC lysozyme assay

Effectiveness of the released lysozyme from PET-based film was performed by HPLC coupled with UV-DAD detection. Chromatography was performed after development and validation of a

RP HPLC method allowing the elution of lysozyme in less than eight minutes. In brief, separation was achieved on a Luna, C18 column (250 mm x 2.0 mm ID), with particle size 5 μ m, from Phenomenex (Castel Maggiore, BO, Italy). Elution was performed by a linear step gradient solvent system consisting of water containing 0.1% (V/V) TFA (eluent A), acetonitrile (eluent B) and changed after the first 2 min from 80% (solvent A): 20% (solvent B) to 50% solvent A: 50% solvent B in 3 min. The elution was performed isocratically for 5 min and then eluent B was increased from 50% to 80% at the flow rate of 0.5 mL/min. The column was thermostated at 45 °C (± 1 °C) and the injected volume was 20 μ l. Monitoring wavelengths were set at 225 nm, 254 nm, and 280 nm. For the quantification of the lysozyme, studies on linearity, precision, selectivity, and recovery were performed, according to Eurachem guidelines (The Fitness for Purpose of Analytical Methods, 1998). Detection limit (y_D) and quantitation limit (y_Q) were preliminarily calculated as signals based on the mean blank (\bar{y}_b) and the standard deviation (s_b) of the blank signals as follows:

$$y_D = \bar{y}_b + 2ts_b$$

$$y_Q = \bar{y}_b + 10s_b$$

where t is a constant of the t-Student distribution (one-sided) depending on the confidence level and the degrees of freedom ($\nu = n-1$; n = number of measurements). Ten blank measurements were performed to calculate \bar{y}_b and s_b . Values of y_D and y_Q were converted from the signal domain to the concentration domain to estimate LOD and LOQ respectively, using an appropriate calibration function.

Linearity was established in the range of concentration between 2.5 and 25 mg L⁻¹ diluting the standard solution. Five equispaced concentration levels were chosen and three replicated injections were performed at each level. The homoschedasticity test was run and the goodness of fit of the calibration curve was assessed applying Mandel's fitting test. A t-test was carried out to verify the significance of the intercept (confidence level 95%). Precision was calculated in terms of inter-day and intra-day repeatability both of area and retention times as R.S.D.% at two concentration levels for analysis.

Intraday repeatability was calculated on peak areas and on retention times using five determinations at two concentration levels in triplicate. Inter-day repeatability was calculated performing the same analyses in two different days.

With the purpose of determine recovery, samples were fortified with the lysozyme at three different levels of concentration, corresponding to the minimum, the maximum and an intermediate value of the linearity range. Percentage of recovery was then calculated with the formula:

$$\text{Recovery (\%)} = (C1-C2)/C3 \times 100$$

where C1 is concentration determined in fortified sample, C2 is concentration determined in unfortified sample and C3 is concentration of fortification.

The release tests were conducted at 4°C (±0.2 °C) and at 25°C ± 1° C (room temperature, RT), under moderate stirring. The small plates of treated PET films (2.5 x 2.0 cm) were put into a Falcon tube and brought in contact with phosphate buffer at pH 6.2.

The lysozyme amount released from films was monitored by taking 0.2 mL from the release test solution at different time intervals (every two hours during 7 days for the samples at RT, and every four hours during 7 days at 4°C) and performing the analysis in triplicate. The release behavior was described from the release data using a relationship derived from the Fick's Law (Bierhalz et al., 2012).

1.2.7. Measure of antimicrobial activity of coatings by turbidimetric lysozyme assay

The activity of lysozyme in solution was determined by measuring the decrease in absorbance with a turbidimetric assay using the method reported by Parry et al. (1965). A suspension of *M. lysodeikticus* (0.2 mg/mL in 50 mM phosphate buffer, pH 6.2) was mixed to the samples to give a final volume of 1 mL. The reaction was allowed to proceed at RT and the decrease in absorbance was monitored at 530 nm for 10 min using UV/VIS spectrophotometer (Perkin–Elmer, Lambda 25, USA). As control, an identical suspension of *M. lysodeikticus*, without addition of lysozyme, has been used, and its absorbance was monitored for 10 min. Specific activity was expressed calculating the slope of the initial linear portion (1.2–3.2 min) of optical density (OD) versus time and dividing these results for the quantity of lysozyme inoculated.

$$[-\Delta\text{OD nm}/\Delta t \text{ min}]/\mu\text{g of lysozyme}$$

The analyses were carried out in triplicate.

1.3. Results and discussion

The sol synthesis and the reagents have been chosen on the basis of a previous work (Minelli et al., 2010) concerning the preparation of hybrid materials starting from the inorganic material TEOS and an organic hydrosoluble polymer (PVOH). These reagents permit to obtain a network formed by crosslinks between the polymeric chains and the inorganic domains, in which lysozyme can be entrapped by physical interactions. The PVOH/TEOS ratio (w/w) was varied from 5% to 35% to obtain a sol which could give an excellent adhesion to the substrate and a good uniformity in the coating structure. The best conditions were obtained using a PVOH/TEOS ratio of 20% (w/w). This mixture was found to be stable in water, in presence of EtOH until 25%, and in a pH range between 2 and 7, which covers the values of most of the food products. The first part of the work was focused on the characterization of the PET polymer surface as obtained after the coating procedure in order to determine its homogeneity, and to control the stability of the coating during a temporary contact with the buffer solution, used as a food simulant. Low temperature plasma treatment of PET supports was used for surface modification and, in particular, for the improvement of its adhesive properties. In terms of adhesion and homogeneity of the coating on the surface of the sample, the best results were obtained by exposing each sample for 30 s to a power of 54 W. After such treatment, as expected, remarkably increase of the PET surface hydrophilicity was observed, enhancing the adhesion properties between PET surface and sol-gel coating containing lysozyme. Structural properties and morphology of the surface polymer obtained after the coating were investigated using ATR infrared

spectroscopy and tapping mode-Atomic Force Microscopy (TM-AFM) measurements.

1.3.1. ATR-FTIR spectra

Figure 8 shows the ATR-FTIR spectra recorded for a PET polymer (A) and for a bare coating obtained by deposition of the sol over a Teflon surface that was gently removed after drying (B). In panel C the ATR-FTIR spectrum taken from the coated PET is displayed. In (A), the characteristic band at the wave number of 1710 cm^{-1} due to ester C=O stretching can be observed (the wave number is lower than that of alkyl esters because of the conjugation with the aromatic ring); the two intense bands around 1238 cm^{-1} and 1090 cm^{-1} can be attributed to O-C-C groups bending in the PET polymer, while two more characteristic bands attributed to the $-\text{CH}_2-$ stretching vibration at 2948 cm^{-1} , and bending (1410 cm^{-1}) are also present. More information were present in the fingerprint region. A band at around 1020 cm^{-1} is related to in-plane vibration of benzene groups, and bands at the wave numbers of about 873 cm^{-1} and 721 cm^{-1} corresponded to out of plane vibration of benzene groups (Vijayakumar and Rajakumar, 2012). The ATR-FTIR spectrum of the bare coating (B) shows the typical broad and intense band at 3300 cm^{-1} , attributed to the O-H stretching of the hydroxyls present in PVOH. Two peaks can be attributed to methylene groups: the peak near to 2950 cm^{-1} , due to C-H stretching, and the weak peak at 1417 , to bending. The broad peak centred at 1052 cm^{-1} can be attributed to the overlapping of the vibration of Si-O-Si groups (1052 cm^{-1}) and of the C-OH bonds (1084 cm^{-1}). The large peak at 955 cm^{-1}

attributed to Si-OH suggests that (as expected) the condensation of silanols was not complete.

The ATR-FTIR spectrum of the coated PET (C) showed the presence of the film deposited; indeed, all the characteristic bands and peaks of the coating are present: the intense and broad band at 3300 cm^{-1} , and the Si-OH peak at 965 cm^{-1} . The peak attributed to the Si-O-Si group at 1052 cm^{-1} appears as a shoulder of the big peak at 1080 cm^{-1} produced by PET. The stability of the coating during 30 days of storage at RT was evaluated by performing three measures (one each ten days). The results obtained did not differ along the whole period.

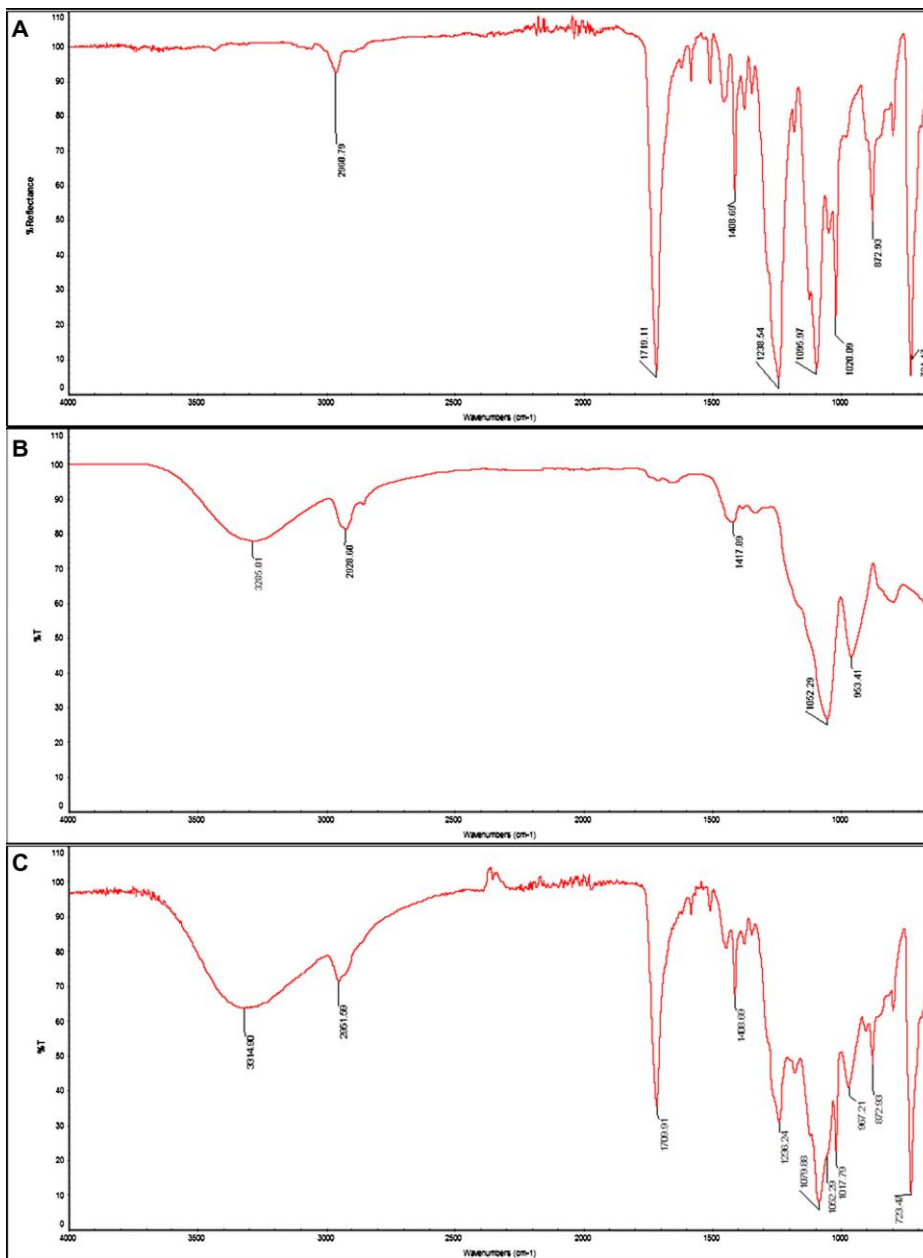


Fig. 8. ATR-FTIR spectra of substrate PET (A), bare coating (B) and coated PET (C).

The stability of the coating during 30 days of storage at RT was evaluated by performing three measures (one each ten days). The results obtained did not differ along the whole period.

1.3.2. Morphology of the films by AFM

A series of morphological assays was performed by tapping-mode AFM. In the AFM the sample is scanned by a sharp tip, which is micromachined onto the end of a cantilever spring. In this way, a topographic image of the sample is obtained by plotting the deflection of the cantilever vs. its position on the sample. Two images of PET films samples are reported in Fig. 9. Panel A shows the image of the coated PET: mean square roughness (Rq) is rather low (± 2 nm) and shows a very flat surface. The parameter Rsk (± 0.3) indicates that the distribution of hills and pits is symmetric and shows that the surface is substantially uniform and maintains the morphology of the substrate. Panel B shows the image of a coated PET sample submitted to an immersion test in phosphate buffer at pH 6.2, at 4°C during 10 days, when the release of lysozyme was shown to be complete (see below). In this sample, the Rq parameter is slightly higher than the previous, showing that the immersion of the sample in the buffer, resulting in the release of the antibacterial, slightly modified the surface morphology of the coating, probably due to a small rearrange of the network.

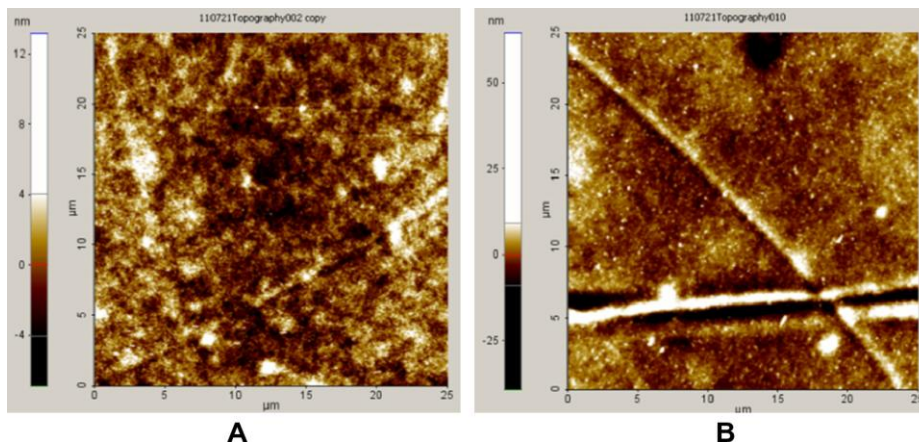


Fig. 9. Images of coated PET films acquired by Force Atomic Microscopy (A, coated PET; and B, coated PET after immersion in buffer solution).

The low R_{sk} value (± 0.5) shows that the surface is substantially uniform, as in the PET film before immersion (see Table 1). All the coated PET samples were submitted to this control procedure and showed similar features. The present data indicate that the film production procedure is reliable and provides good evidence of stability after immersion in buffer solution.

1.3.3. *In vitro* antimicrobial activity of modified packaging

The activity of lysozyme incorporated within the sol–gel modified PET was evidenced by assay in agar plates containing cell walls of *M. lysodeikticus* (Barbiroli et al., 2012; Maehashi et al., 2012; Yua et al., 2013). The appearance of clear inhibition zones both at the contact area and around the plates of coated PET was observed. A qualitative test of inhibition was performed, and a quantitative evaluation was carried out

since the antibacterial activity is proportional to the size of inhibition zone.

Table 1 Calculations of morphological parameters from AFM images: root mean-square roughness (Rq) and Skewness (Rsk).

	Rq mean (nm)	Rsk mean
A (just after film deposition)	2.293 ± 0.313	-0.313 ± 0.016
B (after 10 days of immersion in buffer at 4 °C)	5.113 ± 0.223	-0.462 ± 0.035

Noteworthy, it is possible to modulate the release kinetics by modifying parameters such as temperature and lysozyme concentration, therefore tests were conducted at two temperatures (RT and 4 °C) and at two concentration values. In Fig. 10 the lysis zones obtained at different interval times, with different lysozyme concentration, and at RT or 4 °C, are depicted. A gradual increase in the inhibition zone diameter was observed in all panels, while around controls no halo presence could be observed. In a first set of experiments the amount of lysozyme added to the sol for the preparation of the film was 1.25 mg in 1 mL. When the Petri dishes were incubated at RT a lysis halo with diameter of 24 ± 0.4 mm was obtained after 24 h, while at 4 °C a halo of 12 ± 0.5 mm was visible after 48 h. This result shows that at lower temperatures a lower diffusion rate corresponded, since the matrix is more rigid and the release of the protein is slower. Similar results were obtained by performing the antimicrobial tests on samples obtained employing a lower concentration of lysozyme (0.25 mg of lysozyme in 1 mL of

sol): a lysis halo of 24 ± 0.4 mm, similar in size to that found in the first experiment at 24 h, was observed here only after 48 h with samples incubated at RT, whereas with Petri dishes incubated at 4°C , a lysis halo of 16 ± 0.5 mm was visible after 182 h (corresponding to 7 days). In both experiments conducted at RT, after 7 days, the inhibition zones covered the whole surface of the Petri dish (60 mm). To test if the lysozyme entrapped in the coating could keep its activity during the storage of the film at RT, we repeated the in vitro test after maintaining an aliquot of coated PET along 30 days. The obtained results did not differ from the previous registered.




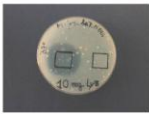


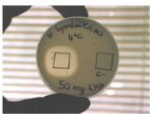
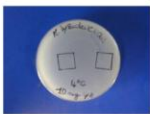
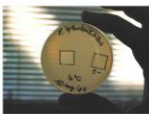
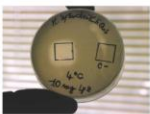
Test Temperature	Lysozyme concentration in the sol	24 h	48 h	182 h (7 days)
RT	1.25 mg/ml			
	0.25 mg/ml			
4°C	1.25 mg/ml			
	0.25 mg/ml			

Fig. 10. Antimicrobial activity on *M. lysodeikticus* at two different temperature (4°C and RT), three time points (24, 48, and 182 h) and two concentration of the lysozyme (0.25 and 1.25 mg/mL). In each Petri dish the squares on the right represent controls, and the squares on the left represent PET treated with coating containing lysozyme.

1.3.4. Kinetic release of lysozyme from coating to a liquid medium

Kinetics of lysozyme release to a liquid medium at pH 6.2 were evaluated by RP-HPLC coupled to UV-DAD detection. Calibration curve was obtained by standard calibration, as illustrated in Section 1.2.6. The linear regression curve showed a correlation coefficient (R^2) over 0.99. The linearity range for lysozyme was established over two orders of magnitude of concentration 2.5–25 mg L^{-1} (Fig. 11). Excellent precision in terms of intraday repeatability was calculated providing RSD% in the 5–6% range for peak areas and 1–2% for migration time ($n = 10$). The intermediate precision results not to exceed 6% for peak areas and 3% for migration times ($n = 10$), confirming good method precision.

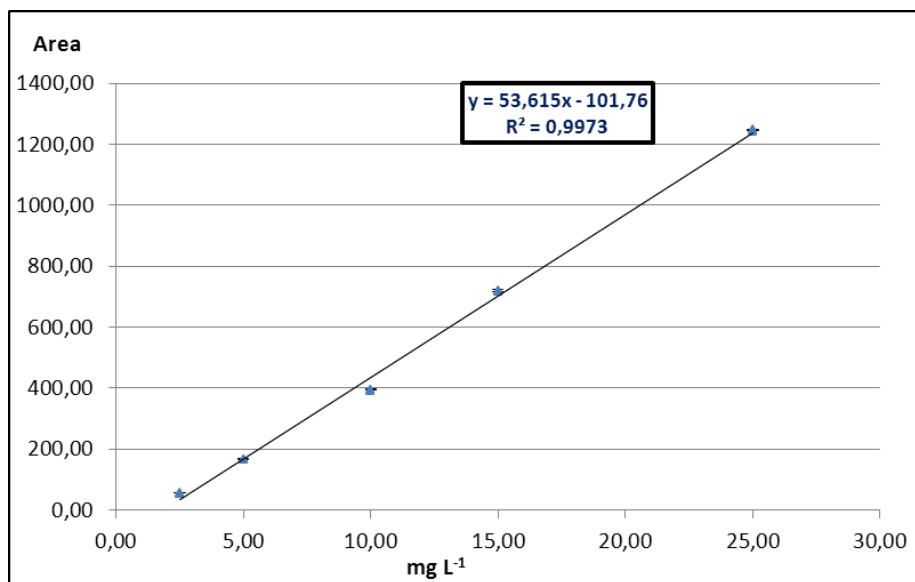


Fig. 11. Lysozyme curve of calibration

At $\lambda=225$ nm, lysozyme showed an LOD and an LOQ, respectively, of 0.30 and 1.00 $\mu\text{g g}^{-1}$. Good results of recovery were obtained with values of $91\pm 5\%$, $95\pm 4\%$, and $96\pm 3\%$, adding the minimum, the maximum and an intermediate value of the linearity range, respectively.

The amounts of released lysozyme vs. time, at 4°C and RT, are reported in Fig. 12. For the samples kept at RT, it can be noticed that the release was completed in 48 h, when lysozyme amount reached the plateau value, while in the test carried out at 4°C the complete release was achieved after 240 h.

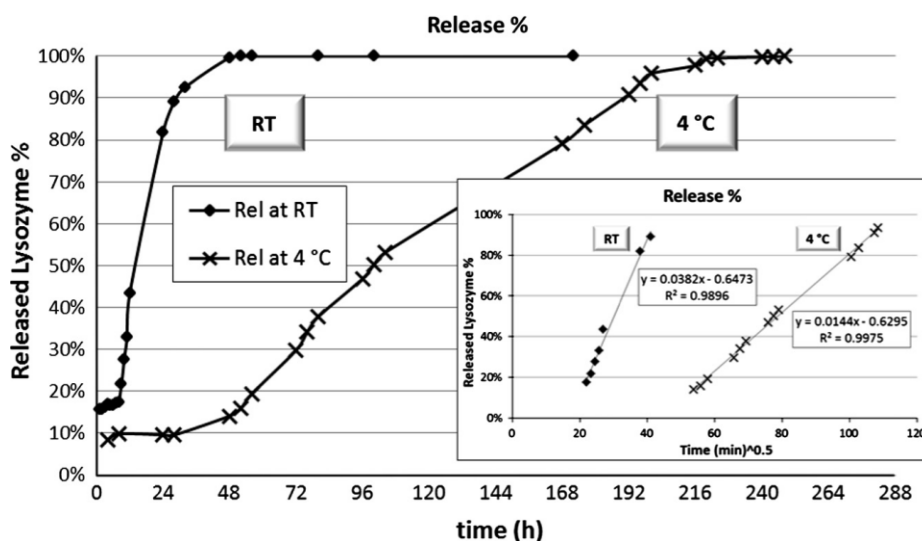


Fig. 12. Lysozyme released from coated PET film. Comparison between amounts of lysozyme in the liquid medium at two different temperatures (RT and 4 °C) as a function of time.

It is possible to detect three different moments in the release process: a lag time where the release does not occur, then a process of diffusion

of the lysozyme, and the final plateau. The release kinetics from systems based on hybrid silica obtained by the sol– gel method have been frequently described (Alfieri et al., 2010) using the Korsmeyer–Peppas model and the semi-empirical equation:

$$F=kt^n$$

where F is the fractional release of the active component, k the kinetic release constant, and t the elapsed time. The n value is related to the geometrical shape of the device and determines the release mechanism (Kosmidis et al., 2003). In presence of a planar releasing surface, n is ½ only with a Fickian diffusion. To verify this hypothesis the fractional release was plotted versus the square root of time (see insert of Fig. 12). As it can be seen, there is an excellent fit in the range 15–90%. The main parameters are summarized in Table 2. The kinetics registered at the two evaluated temperatures shown great differences related to the lag time phase and to the slope.

Table 2 - main parameters of the lysozyme release from the coating at room temperature and at 4 °C

Parameter	RT tests	4°C tests
Lag time	7 hours	28 hours
Kinetic release constant ((min) ^{0.5})	0.038 ±0.002	0.0144 ±0.0002
End of fickian diffusion	28 hours	196 hours
Fractional release at the end of fickian diffusion	87%	93%

In details, a very short lag time is observed at RT, followed by a steep steady increase of the amount of released lysozyme. This datum can be explained considering that the mechanism of release based on the diffusion is determined by a swelling process of PVOH that causes a rearrange of the crosslinking network, allowing the molecules of lysozyme to gain freedom of movement. At lower temperature the mobility of the polymeric chains are assumed to be slowed, making the network more rigid and entrapping lysozyme strongly.

1.3.5. Evaluation of antimicrobial activity of lysozyme released from films

This second microbiological test was carried out to assess the activity of lysozyme after its release from a coated film. In order to verify if the molecule maintained its activity after being entrapped in the coating, its activity was measured and compared to that of a standard solution of the antimicrobial agent at the same concentration. Experiments were carried out following the procedure reported in point 2.7. In Fig. 13, panel A, the kinetic curves of inhibition of *M. lysodeikticus* after the addition of a standard solution of lysozyme at a final concentration of 1.0, 2.0, and 3.0 $\mu\text{g/mL}$ are reported, whereas in panel B the inhibition kinetic curves regarding lysozyme released from antimicrobial films are depicted. The obtained results are summarized in Table 3.

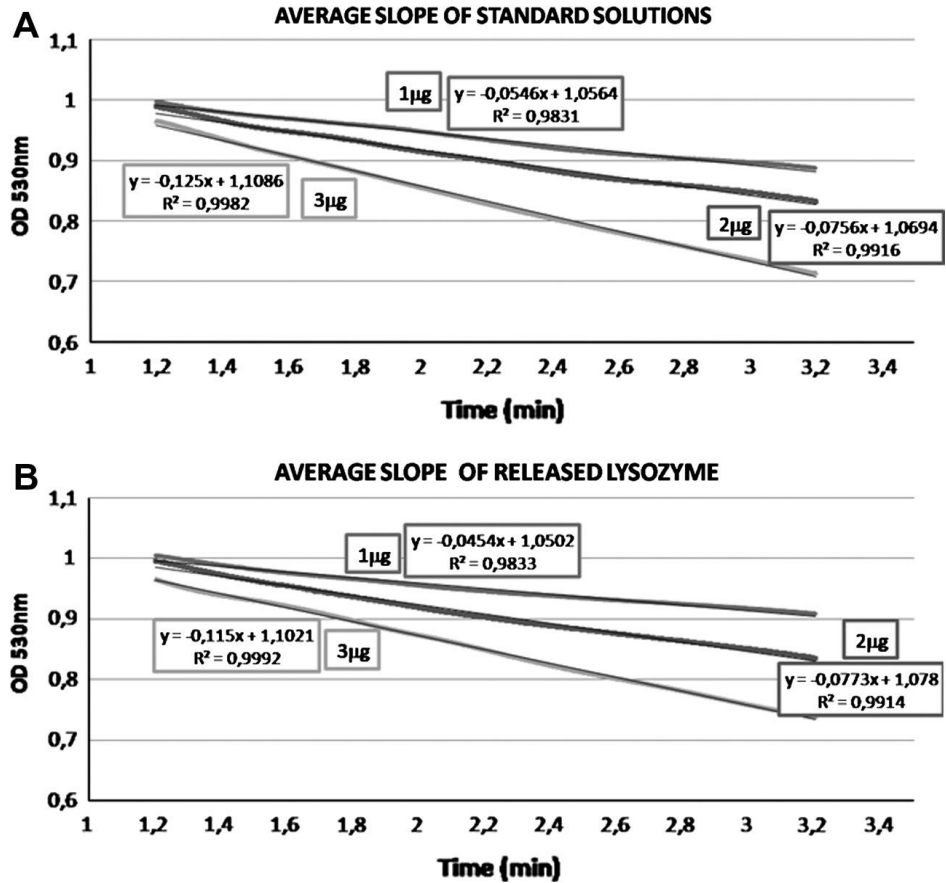


Fig. 13. Turbidimetric assay of standard solution of lysozyme (left) and lysozyme released from coating (right) against *M. lysodeikticus* at three different concentrations. Averaged optical densities for each time were adjusted to a linear regression model.

Comparing the specific activity values derived from slopes it is confirmed that lysozyme from standard solution and antimicrobial released from the coated films exhibit a similar enzymatic activity. The slope of the control (-0.0018 nm/min) shows that without the addition of lysozyme, the absorbance of the suspension of *M. lysodeikticus* did not change.

Table 3. Inhibition activity of lysozyme against *M. lysodeikticus*: standard solutions (A); lysozyme released from a coated film (B).

	LYSOZYME AMOUNT(μg)	AVERAGE SLOPE ($\Delta\text{OD nm}/\Delta t \text{ min}$)	SPECIFIC ACTIVITY (-AV.SLOPE/ amount of lysozyme)	AVERAGE SPEC. ACTIVITY
A	0,9855	-0,0546	0,0552	0,0459
	1,9431	-0,0756	0,0390	
	2,8736	-0,1250	0,0434	
B	0,9855	-0,0454	0,0461	0,0420
	1,9431	-0,0773	0,0398	
	2,8736	-0,1150	0,0400	

1.4. Conclusions

This work shows the optimization of a simple and reproducible procedure for the realization of a new antimicrobial active food packaging. Stable sol–gel hybrid films were prepared by dip-coating on PET substrates previously activated by cold plasma, and were characterized by FT-IR spectroscopy and Atomic Force Microscopy. Lysozyme was employed as antimicrobial agent, and the activity of the enzyme fixed on the substrate was confirmed by tests performed on plates containing *M. lysodeikticus*.

Release tests were carried out verifying that lysozyme migrated from the film to water solution with a temperature-dependent rate. The enzymatic activity kinetics of the solution of lysozyme released showed that the enzyme still kept its activity after being incorporated onto the film. Furthermore, a novelty of this approach relies in the possibility to modulate the release of the active substance by adjusting the relative amount of reagents employed through a modification of the crosslinks between the polymeric chains and the inorganic domains. The obtained films present the main characteristics to be proposed as possible innovative antimicrobial food packaging. Further studies are encouraged to be performed in order to test this new active packaging on food products.

1.5. References

Alfieri, I., Lorenzi, A., Montenero, A., Gnappi, G., and Fiori, F., 2010. Sol-gel silicon alkoxides–polyethylene glycol derived hybrids for drug delivery systems. *Journal of Applied Biomaterials and Biomechanics*, 8, 14–19.

Anthierens, T., Ragaert, P., Verbrugge, S., Ouchchen, A., De Geest, B.G., Nosedà, B., Mertens, J., Beladjal, L., De Cuyper, D., Dierickx, W., Du Prez, F., and Devliegher, F., 2011. Use of endospore-forming bacteria as an active oxygen scavenger in plastic packaging materials. *Innovative Food Science and Emerging Technologies*, 12, 594–599.

Appendini, P., and Hotchkiss, J.H., 2002. Review of antimicrobial food packaging. *Innovative Food Science and Emerging Technologies*, 3, 113–126.

Barbiroli, A., Bonomi, F., Capretti, G., Iametti, S., Manzoni, M., Piergiovanni, L., and Rollini, M., 2012. Antimicrobial activity of lysozyme

and lactoferrin incorporated in cellulose-based food packaging. *Food Control*, 26, 387–392.

Bierhalz, A.C.K., da Silva, M.A., and Kieckbusch, T.G., 2012. Natamycin release from alginate/pectin films for food packaging applications. *Journal of Food Engineering*, 110, 18–25.

Buonocore, G.G., Del Nobile, M.A., Panizza, A., Bove, S., Battaglia, G., and Nicolais, L., 2003. Modeling the lysozyme release kinetics from antimicrobial films intended for food packaging applications. *Journal of Food Science*, 68, 1365–1370.

Buonocore, G.G., Conte, A., Corbo, M.R., Sinigaglia, M., and Del Nobile, M.A., 2005. Mono and multilayer active films containing lysozyme as antimicrobial agent. *Innovative Food Science and Emerging Technologies*, 6, 459–464.

Coma, V., and 2008. Bioactive packaging technologies for extended shelf life of meatbased products. *Meat Science*, 78, 90–103.

Conte, A., Buonocore, G.G., Sinigaglia, M., and Del Nobile, M.A., 2007. Development of immobilized lysozyme based active film. *Journal of Food Engineering*, 78, 741–745.

de Azeredo, H.M.C., 2013. Antimicrobial nanostructures in food packaging. *Trends in Food Science & Technology*, 30, 56–69.

de Souza, P.M., Fernandez, A., Lopez-Carballo, G., Gavara, R., and Hernandez-Munoz, P., 2009. Modified sodium caseinate films as releasing carriers of lysozyme. *Food Hydrocolloids*, 24, 300–306.

Gemili, S., Yemenicioglu, A., and Altinkaya, S.A., 2009. Development of cellulose acetate based antimicrobial food packaging materials for controlled release of lysozyme. *Journal of Food Engineering*, 90, 453–462.

Gucbilmez, C.M., Yemenicioglu, A., and Arslanoglu, A., 2007. Antimicrobial and antioxidant activity of edible zein films incorporated with lysozyme, albumin proteins and disodium EDTA. *Food Research International*, 40, 80–91.

Han, J.H., 2000. Antimicrobial food packaging. *Food Technology* 54, 56–65.

Hauser, C., Wunderlich, J., 2011. Antimicrobial packaging films with a sorbic acid based coating. *Procedia Food Science* 1, 197–202.

Hanušová, K., Šťastná, M., Votavová, L., Klaudivová, K., Dobiáš, J., Voldřich, M., and Marek, M., 2010. Polymer films releasing nisin and/or natamycin from polyvinylchloride lacquer coating: Nisin and natamycin migration, efficiency in cheese packaging *Journal of Food Engineering*, 99, 491-496.

Kerry, J.P., O’Grady, M.N., and Hogan, S.A., 2006. Past, current and potential utilisation of active and intelligent packaging systems for meat and muscle-based products: a review. *Meat Science*, 74, 113–130.

Kosmidis, K., Rinaki, E., Argyrakakis, P., and Macheras, P., 2003. Analysis of Case II drug transport with radial and axial release from cylinders. *International Journal of Pharmaceutics*, 254, 183–188.

La storia, A., Ercolini, D., Marinello, F., and Mauriello, G., 2008. Characterization of bacteriocin – coated antimicrobial polyethylene films by atomic force microscopy. *Toxicology and Chemical Food Safety*, 79 (4), 48–54.

Lie, O., Syed, M., and Solbu, H., 1986. Improved agar plate assays of bovine lysozyme and haemolytic complement activity. *Acta Veterinaria Scandinavica*, 27, 23–32.

Maehashi, K., Matano, M., Irisawa, T., Uchino, M., Kashiwagi, Y., and Watanabe, T., 2012. Molecular characterization of goose- and chicken-type

lysozymes in emu (*Dromaius novaehollandiae*): evidence for extremely low lysozyme levels in emu egg white. *Gene*, 492 (1), 244–249.

Manso, S., Cacho-Nerin, F., Becerril, R., and Nerina, C., 2013. Combined analytical and microbiological tools to study the effect on *Aspergillus flavus* of cinnamon essential oil contained in food packaging. *Food Control*, 30, 370-378.

Marini, M., De Niederhausern, S., Iseppi, R., Bondi, M., Sabia, C., Toselli, M., and Pilati, F., 2007. Antibacterial Activity of Plastics Coated with Silver-Doped Organic-Inorganic Hybrid Coatings Prepared by Sol Gel Processes. *Biomacromolecules*, 8, 1246-1254.

Mastromatteo, M., Lecce, L., De Vietro, N., Favia, P., and Del Nobile, M.A., 2011. Plasma deposition processes from acrylic/methane on natural fibres to control the kinetic release of lysozyme from PVOH monolayer film. *Journal of Food Engineering*, 104, 373–379.

McMillin, K.W., 2008. Where is MAP Going? A review and future potential of modified atmosphere packaging for meat. *Meat Science*, 80, 43–65.

Mecitoglu, C., Yemenicioglu, A., Arslanoglu, A., Seda Elmacı, Z., Korel, F., and Emrah Cetin, A., 2006. Incorporation of partially purified hen egg white lysozyme into zein films for antimicrobial food packaging. *Food Research International*, 39, 12–21.

Minagawa, S., Hikima, J., Hirono, I., Aoki, T., and Mori, H., 2001. Expression of Japanese flounder c-type lysozyme cDNA in insect cells. *Developmental and Comparative Immunology*, 25, 439–445.

Minelli, M., De Angelis, M.G., Doghieri, F., Rocchetti, M., and Montenero, A., 2010. Barrier properties of organic–inorganic hybrid coatings based on polyvinyl alcohol with improved water resistance. *Polymer engineering and Science*, 50, 144–153.

Muriel-Galet, V., López-Carballo, G., Gavara, R., and Hernández-Muñoz, P., 2012. Antimicrobial food packaging film based on the release of LAE from EVOH. *International Journal of Food Microbiology*, 157, 239–244.

Parry Jr., R.M., Chandan, R.C., and Shahani, K.M., 1965. A rapid and sensitive assay of muramidase. *Experimental Biology and Medicine*, 119 (2), 384–386.

Proctor, V.A., and Cunningham, F.E., 1988. The chemistry of lysozyme and its use as a food preservative and a pharmaceutical. *Critical Reviews in Food Science and Nutrition*, 26, 359–395.

Quintavalla, S., and Vicini, L., 2002. Antimicrobial food packaging in meat industry. *Meat Science*, 62, 373–380.

Seydim, A.C., and Sarikus, G., 2006. Antimicrobial activity of whey protein based edible films incorporated with oregano, rosemary and garlic essential oils. *Food Research International*, 39, 639–644.

Soto-Cantu, C.D., Graciano-Verdugo, A.Z., Peralta, E., Islas-Rubio, A.R., Gonzalez-Cordova, A., Gonzalez-Leon, A., and Soto-Valdez, H., 2008. Release of butylated hydroxytoluene from an active film packaging to Asadero cheese and its effect on oxidation and odor stability. *Journal of Dairy Science*, 91, 11–19.

Suppakul, P., Miltz, J., Sonneveld, K., and Bigger, S.W., 2003. Active packaging technologies with an emphasis on antimicrobial packaging and its application. *Journal of Food Science*, 68, 408–420.

Suppakul, P., Sonneveld, K.S.W., and Miltz, J., 2011. Diffusion of linalool and methylchavicol from polyethylene-based antimicrobial packaging films. *Food Science and Technology*, 44, 1888–1893.

Sunga, S.Y., Sina, L.T., Tee, T.T., Bee, S.T., Rahmat, A.R., Rahman, W.A.W.A., Tan, A.C. and Vikhraman, M., 2013. Antimicrobial agents for food packaging applications. *Trends in Food Science & Technology*, 33, 110-123.

The Fitness for Purpose of Analytical Methods, 1998. A Laboratory Guide to Method Validation and Related Topics, Eurachem Guide, 1st English edition 1.0, LGC (Teddington) Ltd., <<http://www.eurachem.org/>>.

Vermeiren, L., Devlieghere, F., van Beest, M., de Kruijf, N., and Debevere, J., 1999. Developments in the active packaging of foods. *Trends in Food Science and Technology*, 10, 77–86.

Vijayakumar, S., and Rajakumar, P.R., 2012. Infrared spectral analysis of waste pet samples. *International Letters of Chemistry, Physics and Astronomy*, 4, 58–65.

Wang, S., Marcone, M.F., Barbut, S., Lim and Loong-Tak, 2012. Fortification of dietary biopolymers-based packaging material with bioactive plant extracts. *Food Research International*, 49, 80–91.

Yua, L., Suna, B., Li, J., and Suna, L., 2013. Characterization of a c-type lysozyme of *Scophthalmus maximus*: expression, activity, and antibacterial effect. *Fish and Shellfish Immunology*, 34, 46–54.

Chapter 2

Based on:

Natamycin based sol-gel antimicrobial coatings on polylactic acid films for food packaging

By:

Lantano, C., Alfieri, I., Cavazza, A., Corradini, C., Lorenzi, A.,
Zucchetto, N., Montenero, A.

Submitted to *Food Chemistry*

2.1. Introduction

Natamycin (NAT) (also known as piramicin) is a macrolide polyene (Fig. 1) antifungal antibiotic product of *Streptomyces* species during fermentation, in particular from actinomycete *Streptomyces natalensis* and also from *Streptococcus* species, specifically *Streptococcus lactis* (Chen et al., 2008). This compound is approved by the Food and Drug Administration (FDA) as a food additive and deemed to be a GRAS (Generally Regarded As Safe), and is assigned to be the number E-235-natural preservative in European Union (Ture et al., 2008).

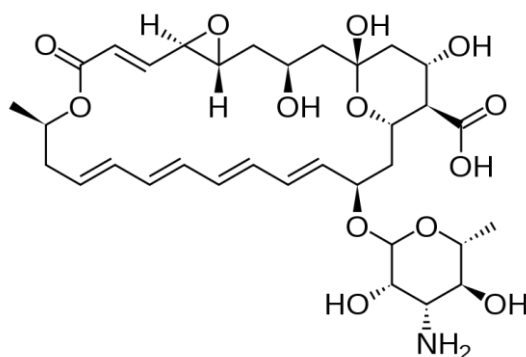


Fig. 1. Chemical structure of Natamycin

The most popular use of this additive, according to the 95/2/EC directive, is the spray directly over the semi-hard and semi-soft cheese and dry, cured sausage at maximum level of 1 mg/dm² in the outer 5 mm of the surface. A limit of this practice is the bad control of the deposited amount with the quick initial diffusion into the bulk of food

(Quattara et al., 2000), reducing the protection in the surface (Appendini and Hotchkiss, 2002). Several studies reported that this active agent can be incorporated inside polymeric packaging by casting process (de Oliveira et al., 2007; Zactiti and Kieckbusch, 2009; Bierhalz et al., 2012; Bierhalz et al., 2013) or deposited onto plastic film surface (Hanušova et al., 2010).

Following a sol gel methodology is possible to obtain an inorganic oxidic network in which the amount of antifungal put in contact with the food product can be controlled, and its eventual release from the film can be modulated by choosing the more opportune coating composition. In particular, preliminary studies suggested that the percentage of the organic component affects the migration of the active substance into food.

The goal of this study was to develop for the first time an antimicrobial coating obtained by sol-gel technique and deposited on commercial polylactic acid (PLA) substrates, in which NAT is physically entrapped.

PLA (Fig.1) was chosen as it represents an innovative material, characterized by being biodegradable, and known to be suitable for food packaging (Koide and Shi, 2007); it also shows good mechanical properties and high resistance, and has been recently successfully employed for active food packaging (Mascheroni et al., 2013).

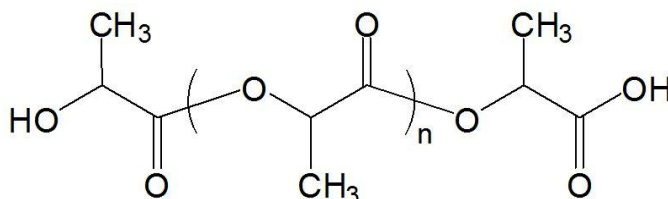


Fig.2. Chemical structure of PLA

The effect of organic-inorganic O/I ratio (defined as the PVOH/TEOS ratio), was evaluated with the aim of avoiding the possible migration of NAT to food. Indeed, it has been considered that the amount of NAT eventually transferred to the food should be limited as much as possible, by employing the lowest active concentration in order to prevent possible immune-resistance effects on the consumer (Delves-Broughton et al., 2005). The migration of antifungal was experimentally measured by HPLC-DAD (Guarino et al., 2011) and mathematically modeled, by following the Regulation EU 10/2011 requiring the employment of water and ethanol 50:50 v/v as food simulating liquid for processed cheese. Besides, the antimycotic property of the film was investigated by testing the films on the surface of commercial semi-soft cheese according to the procedure followed by previous studies (Fajardo et al., 2010; Hanušova et al., 2010; Kallinteri et al., 2013).

2. 2. Materials and methods

2.2.1. Materials

PVOH (MW=88,000-97,000, Alfa Aesar, Karlsruhe, Germany), tetraethoxysilane (TEOS, $\geq 99,0\%$ (GC), Fluka), hydrochloric acid (37%, v/v, Riedel-de-Haën); natamycin, ethanol (absolute), trifluoroacetic acid (spectrophotometric grade) and acetonitrile (HPLC grade) from Sigma Aldrich, Gallarate, Italy; deionized water ($< 18 \text{ M}\Omega \text{ cm}$ resistivity, Milli-Q element water purification system, Millipore, Bedford, USA), soft cheese (local supermarket); polylactic acid (Taghleef Industries SpA, Udine, Italy).

2.2.2. Coatings preparation

The active coatings were obtained by sol-gel technique: sols were prepared employing PVOH, as plasticizer, dissolved in distilled water at 84 °C for 1 h and mixed under continuous magnetic stirring in a tightly closed bottle to prevent evaporation. The inorganic Si-O-Si groups were obtained by addition of TEOS (Montenero, et al., International Patent, 2007). Four sols at different ratio of PVOH/TEOS were studied and named A ($r=1/19$), B ($r=1/9$), C ($r=1/6$), D ($r=1/4$).

To catalyze the hydrolysis and condensation reactions, the solutions were adjusted by adding a small amount of HCl. In these conditions, the components reacted according to the classical sol-gel route (Minelli et al., 2010). The sols were stirred at room temperature for 1 h before adding the natamycin (two concentrations were used: 0.625 mg/mL and 1.25 mg/mL) and ethanol, which was used to improve the active agent solubility in water; the silicon concentration was fixed at 0.5M. All mixtures were stirred by magnetic bar until the active substance was homogeneously dispersed. Another sol without PVOH was prepared. A quote of sol without NAT was also prepared for negative controls.

The PLA films were treated with cold plasma by “Colibri” by Gambetti Vacuum Srl that works within the absolute pressure range of 0.1–1 mbar. The plasma treatment was performed for 20 s in air at 54 W. The sol was deposited on the activated PLA by dip-coating process at a constant speed of 7.0 cm/min and then they were dried in oven at 30 °C ($\pm 1^\circ\text{C}$) for 10 minutes.

To evaluate the amount of natamycin incorporated in the coating, a procedure based on weight variations was carried out using analytical balance. In detail, PLA substrates having known surface were weighted

before and after the coatings formation, obtaining the coating/surface ratio in mg/dm² for each sol. Before, the sol density (mg/ml) and the sol solid content (g of solid after the thermal treatment/ g of sol) for every sol were calculated. All the measurements were in triplicate. The natamycin amount was then calculated by NAT sol concentration (mg/ml) and sol deposited (ml/dm²), using the formulas below:

$$\text{deposited sol} \left(\frac{\text{volume}}{\text{surface}} \right) = \frac{\text{deposited Coating} \left(\frac{\text{weight}}{\text{surface}} \right)}{\text{sol solid content} \left(\frac{\text{weight}}{\text{weight}} \right) \times \text{sol density} \left(\frac{\text{weight}}{\text{volume}} \right)}$$

$$\text{natamycin in the coating} \left(\frac{\text{weight}}{\text{surface}} \right) = \text{natamycin sol concentration} \left(\frac{\text{weight}}{\text{volume}} \right) \times \text{deposited sol} \left(\frac{\text{volume}}{\text{surface}} \right)$$

2.2.3. Fourier-transform infrared spectroscopy

IR spectra were acquired using the Nicolet iS50 FT-IR Spectrometer with Pike Smart MIRacle™ single reflection horizontal ATR (HATR) attachment containing a flat and polished diamond/ZnSe sandwich crystal of 2 mm crystal, using OMNIC software (all from Thermo Fisher, Milan, Italy).

Ethanol absolute was used to clean the ATR crystal prior to the first spectral analysis of each sample.

HATR-IR is a useful way of analyzing solid samples without the need for cutting samples. Infrared spectra were taken in the spectral range from 4000 to 650 cm⁻¹; the samples analyzed are: PLA TQ, PLA with

SiO₂ coating and 4 samples of PLA with different coatings (CoA, CoB, CoC and CoD from sol A, B, C and D respectively).

2.2.4. Activity evaluation of natamycin coatings in contact with cheese sample

The evaluation of film antimicrobial activity and the determination of the optimum natamycin concentration were carried out on commercial soft cheese. PLA strips (3 x 6 cm) treated with each sol were put over slices of cheese (1 cm of thickness). All cheese samples were placed on plastic trays and were covered with a perforated aluminium foil to guarantee internal oxygenation for fungus growth (de Oliveira et al., 2007). They were incubated up to 30 days at 4 °C in a refrigerator to reproduce as much as possible the typical shelf life storage conditions of cheese. The efficiency was evaluated on the basis of moulds growth under the film (Fajardo et al., 2010). A coating prepared without addition of NAT was used as control. The other cheese samples were covered with coatings A, B, C, and D and with coating A with low amount of NAT (0.09 mg/dm²). The assays were performed in triplicate.

2.2.5 Release of natamycin from coated films to food simulant

PLA coated films of 120 cm² (± 0.2) area were cut into 3 x 2.5 cm pieces and immersed in 20 mL of ethanol/water solution 50% (v/v) at a temperature of 4°C (± 0.2 °C) under stirring (Corradini et al., 2013). 100 µL of this solution were taken out at different time intervals during

15 days to determine natamycin released from films and they were injected in the HPLC-DAD system.

The analyte was separated on a Luna C18 column (250 mm x 2.0 mm ID) with particle size 5 μ , from Phenomenex. Analyte was separated using 0.1% trifluoroacetic acid (TFA) in water (v/v) as eluent A, and 0.1% TFA in acetonitrile (v/v) as eluent B. An isocratic step consisting in 40% of phase B for 7 min was employed. The flow rate was 0.2 mL/min, the working temperature of the column was set to 30 °C and the injected volume was 20 μ l. The wavelength of the photodiode array UV detector was set at 303 nm.

For the quantification of NAT, studies on LOD, LOQ, linearity, precision, selectivity, and recovery were performed, according to Eurachem guidelines (The Fitness for Purpose of Analytical Methods, 1998) as reported in Chapter 1 (Section 1.2.6.).

2.3. Results and discussion

2.3.1. Chemical and physical characterization of the films

The goal of the first step of this work was to find the best conditions to improve the coating properties by enhancing its resistance and stability, and controlling the amount of antifungal entrapped. For this purpose, the evaluation of the effect of organic-inorganic O/I ratio in the sol was investigated, since the percentage of organic component has been found to be responsible for the amount of active substance incorporated, and also for its stability inside the film obtained (Buonocore et al., 2005).

The study was carried out by preparing four different sols with O/I ratio equal to 1/19 (sol A), 1/9 (sol B), 1/6 (sol C) and 1/4 (sol D). The

sols were prepared employing a constant concentration of active substance (1.25 mg/mL), and were deposited on the PLA substrates by dip coating at specific velocity obtaining samples coated on both sides. The coatings obtained in this way were colorless and perfectly transparent. Previously, due to its hydrophobic nature, PLA was treated with cold plasma before deposition to improve adhesion; the best time-tested is 20 s in term of homogeneity of sol deposition and consequent adhesion. After a 0.5 s longer plasma treatment the PLA surface resulted completely stressed. All the sol-gel active coatings on polylactic acid films were submitted to morphological assays by AFM, showing that uniform coated surfaces were obtained, as previously reported (Corradini et al., 2013).

Table 1 shows the results related to the amount of natamycin incorporated in the four different preparations. As can be observed, the weight of gel attached to the film was higher when PVOH was in higher proportion. The data can be explained taking into account that the viscosity of the medium increases with the increasing of PVOH percentage. According to Landau-Levich law, in a dipping process the thickness of the coating directly grows with viscosity, so working always at the same withdrawal rate, it is reasonable to suppose that the weight increases as reported.

Table 1. List and characteristics of the examined samples^a

Coating Name	O/I ratio	Coating mg/dm ²	Solid content (w/w)	SOL density mg/mL	NAT mg/dm ²
CoA	1/19	6.2±0.4	0.046±0.006	942±9	0.18±0.04
CoB	1/9	8.4±0.9	0.047±0.007	970±40	0.23±0.07
CoC	1/6	15.3±0.9	0.0614±0.0002	950±20	0.33±0.03
CoD	1/4	29±1	0.066±0.005	980±30	0.56±0.09

^a Average ± standard deviation of experimental determination (n=3)

On other hand, from the data shown in Table 1 it can be seen that in all cases the amount of NAT deposited on the PLA surface was significantly lower than that allowed on the surface of the rind of cheese, i.e. 1 mg/dm², according to Directive 95/2/EC.

2.3.2. ATR-FTIR spectra

Structural properties and morphology of the surface polymers obtained after the coating deposition were investigated using ATR infrared spectroscopy measurement. Figure 3 shows the ATR-FTIR spectra recorded for a PLA film (A), PLA with SiO₂ coating (B) and a stack of 4 coatings with same composition but different O/I ratio (C).). In Table 2 the wavenumbers (cm⁻¹) and vibrational assignments of PLA are reported.

Table 2. ATR-IR peaks and vibrational assignments

ATR-IR peaks	Assignments
3002-2947 cm^{-1}	Stretching CH_3 (s + as)
1746 cm^{-1}	Stretching $\text{C}=\text{O}$
1450 cm^{-1}	Bending CH_3 (as)
1381-1362 cm^{-1}	Bending $\text{CH} + \text{CH}_3$ (s)
1263 cm^{-1}	Bending $\text{CH} +$ Stretching COC
1185 cm^{-1}	Stretching COC (as)
1128 cm^{-1}	Rocking CH_3 (as)
1077 cm^{-1}	Stretching COC (s)
1043 cm^{-1}	Stretching $\text{C}-\text{CH}_3$
958 cm^{-1}	Rocking $\text{CH}_3 +$ Stretching CC
866 cm^{-1}	Stretching $\text{C}-\text{COO}$
753 cm^{-1}	Bending $\text{C}=\text{O}$

Panel I shows the typical spectrum of PLA: peak at 1746 cm^{-1} is given by the stretching of $\text{C}=\text{O}$; the 1185 and 1077 cm^{-1} bands are respectively attributable to $\text{C}-\text{O}-\text{C}$ asymmetric and symmetric stretchings. 1128 cm^{-1} peak is ascribable to $\text{C}-\text{H}$ (of CH_3 groups) rocking mode, while the peak at 1043 cm^{-1} is caused by $\text{C}-\text{CH}_3$ stretching.

Spectra reported in panels II and III show small differences in comparison with the previous. In these spectra a new weak band near to 3300 cm^{-1} is visible, imputable to the stretching of OH groups present in the coatings (SiOH and PVOH). The peak of the $\text{Si}-\text{O}-\text{Si}$ (1052 cm^{-1}) is not distinguishable, being covered by the broad band ($1080-1040 \text{ cm}^{-1}$) produced by PLA bonds (Weng et al., 2013). In Panel III, OH band (3300 cm^{-1}) becomes more intense with increasing the PVOH percentage (from CoA to CoD); the other PVOH peaks (region around $1450-1040 \text{ cm}^{-1}$) overlap with the PLA ones determining broad bands; at the same time, as expected, the relative

intensity of these bands compared to the 1742 cm^{-1} band of the substrate become higher.

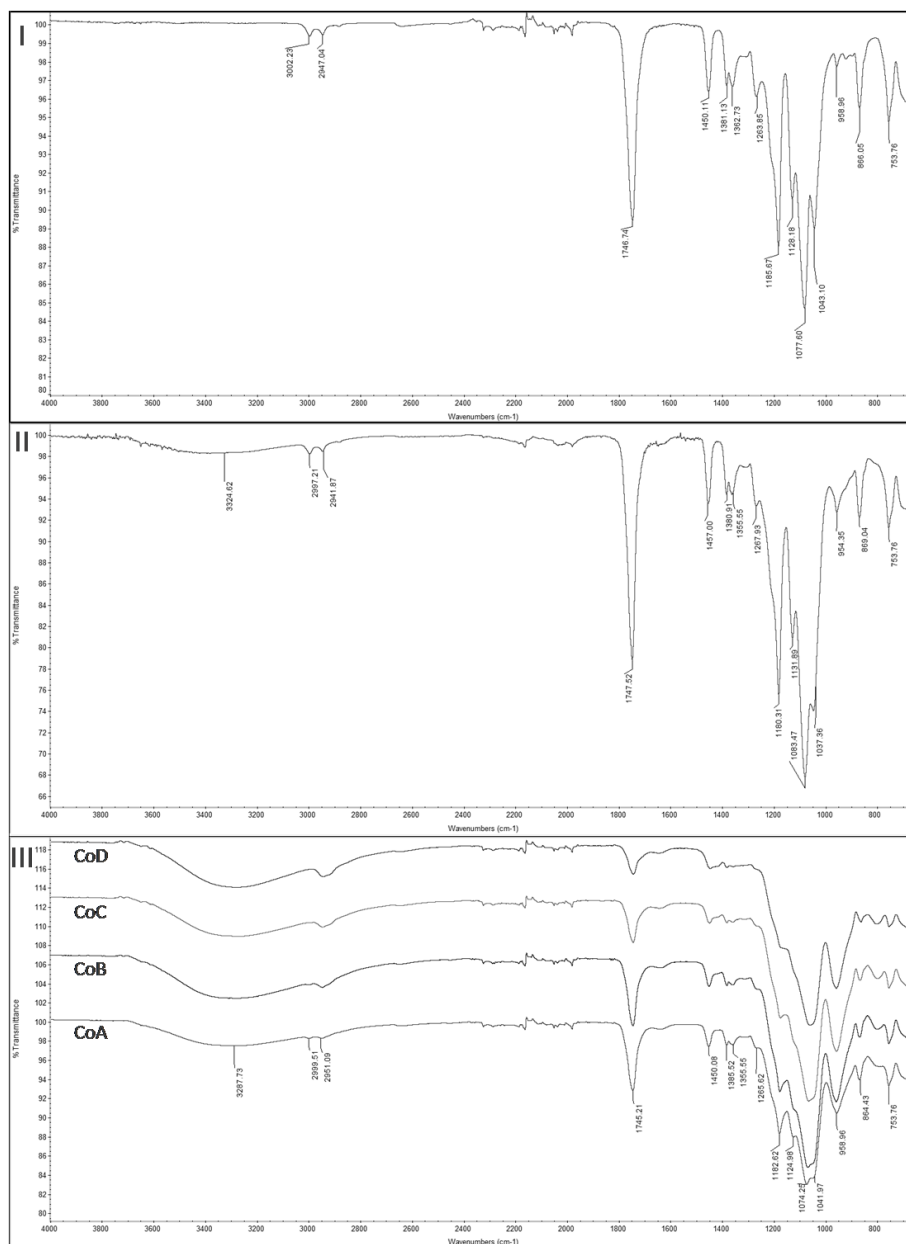


Fig. 3. ATR-FTIR spectra recorded for a PLA film (I), PLA with SiO₂ coating (II) and a stack of 4 coatings with same composition but different O/I ratio (III).

2.3.3. Tests of mould growth on cheese samples

In order to verify the inhibitory effect of NAT entrapped into coatings, strips of functionalized PLA were put in contact with cheese surfaces (Gonzales et al., 2013). This procedure has been chosen instead of a direct measurement over agar plates because, due to the higher water content, it could change the properties of coatings and the NAT release (Fajardo et al., 2010).

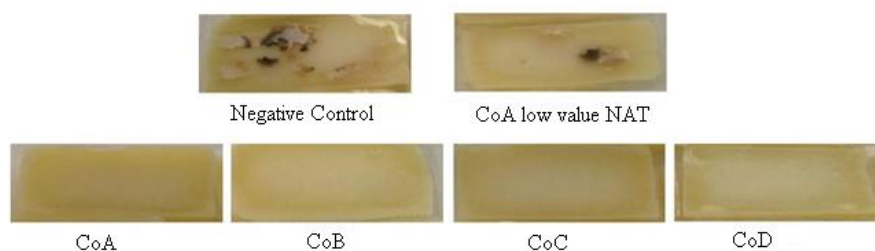


Fig. 4. Comparison between cheese samples stored in active packaging after incubation at 4 °C during 30 days: negative control, coating A with low value (halved) of NAT; coating A, B, C and D.

As shown in Figure 4, related to cheese samples after 30 days of incubation at 4 °C, the strips CoA, CoB, CoC and CoD inhibited the mould growth, in contrast to the negative control showing the appearance of relevant mould growth. The inhibitory effect was observed for all O/I ratio studied, correspondent to different amounts of NAT entrapped (see Table 1), and no sensible effects of NAT concentration could be observed in the range covered by this series of experiments. On the other hand, when NAT concentration was reduced

to 50% (CoA low value NAT), the mould growth was not completely inhibited, demonstrating that the effect is dependent on NAT concentration. Therefore, this last coating proved to be inefficient to be employed for cheese storage. Between all samples examined, CoA can be considered ideal, as it contains the lowest amount still active.

2.3.4. Release of natamycin from films

The amount of NAT released from coatings was tested by employing a solution of EtOH/H₂O=50/50 (v/v), chosen as food simulant liquid for fatty food as cheese, according to European Regulation (10/2011). Quantitative measurements were carried out by RP-HPLC coupled to UV-DAD detection, The retention time was 5,5 minute for NAT (Fig. 5). Using 303 nm as detection wavelength, the calibration curve of NAT was linear from 0.05 to 10 µg/mL (Fig. 6). The limit of detection and quantitation, LOD and LOQ, were found to be 0.03 and 0.05 µg/mL respectively. The CV% for precision in term of repeatability (intraday) was evaluated and found to be less than 6% for peak areas and 0.3 % for migration time (n = 9). The intermediate precision (interday repeability) was shown to be not exceeding 13% and 1% for the peak areas and for migration times (n = 15) respectively. The results indicated that the method has good precision. Correlation coefficient was found to be over 0.99.

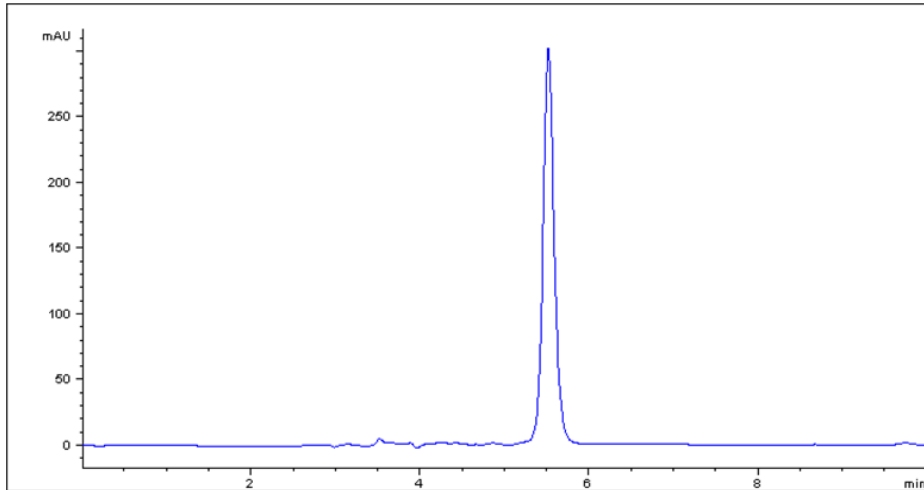


Fig. 5. The RP-HPLC elution profile of released natamycin from coating D after 48 hours

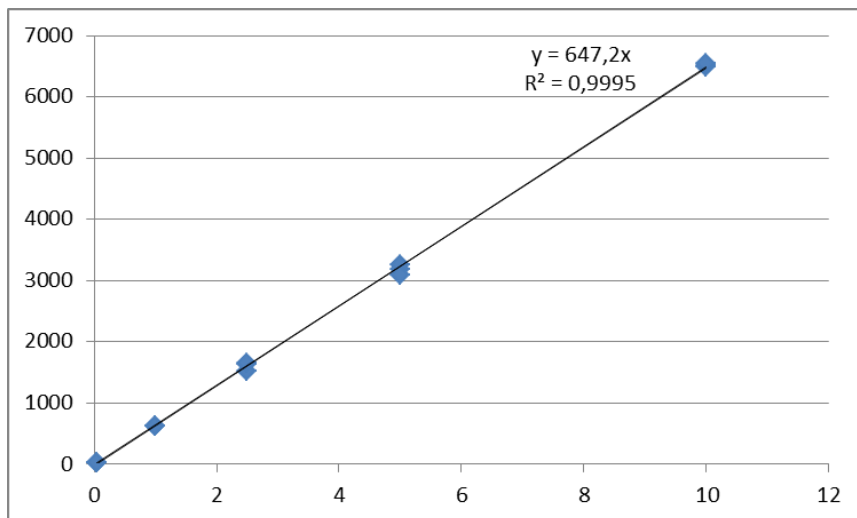


Fig. 6. Natamycin curve of calibration

The kinetics of released NAT from four different coatings (CoD, CoC, CoB and CoA) into food simulant liquid vs. time at 4 °C are reported in Fig. 7.

As shown, for each coating, a process of diffusion of NAT (solid line) and a final plateau can be observed, illustrating that the initial release characteristics followed a Fickian behavior due to the release of uniformly distributed antimicrobial agent, as reported in the Chapter 1 (Section 1.3.4.). For each coating, the main parameters are shown in Table 3.

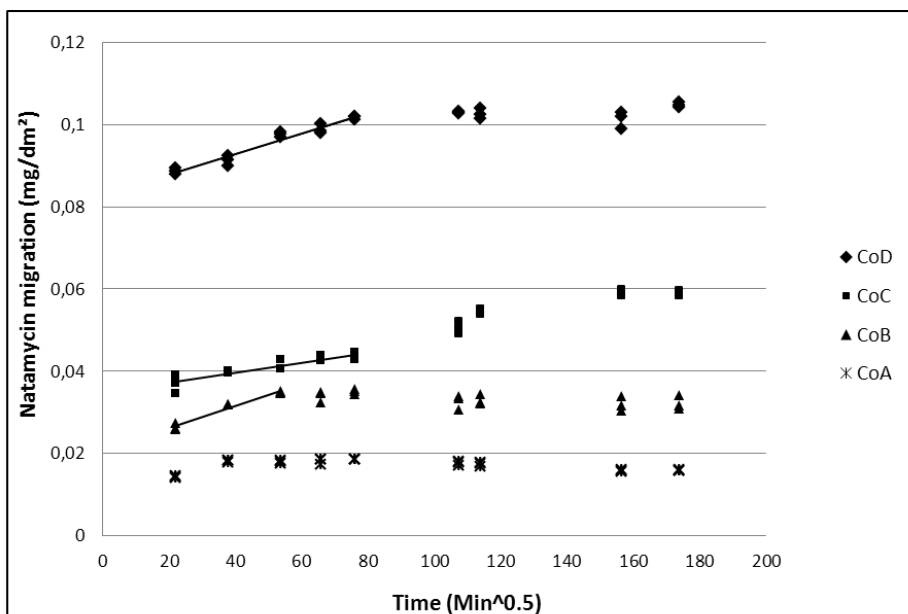


Fig. 7. The course of natamycin migration from four coatings (CoA, CoB, CoC and CoD with O/I ratio equal to 1/19, 1/9, 1/6 and 1/4 respectively) into EtOH/H₂O=50/50 (v/v) at 4°C. The NAT fickian diffusions from coatings are represented by the solid lines.

Table 3. Main parameters of the natamycin release from the coating at different O/I ratio at 4°C

Coating	Kinetic release constant ((min) ^{0.5})	End of fickian diffusion (h)	R ²
CoA	/	/	/
CoB	$2.6 \times 10^{-4} \pm 0.2 \times 10^{-4}$	48	0.971
CoC	$1.24 \times 10^{-4} \pm 0.16 \times 10^{-4}$	96	0.917
CoD	$2.48 \times 10^{-4} \pm 0.16 \times 10^{-4}$	96	0.976

A comparison between the kinetics registered for each coating indicates that maximum NAT release from CoA was achieved after 24h. The NAT in CoB was depleted in 48 h, in 96 h for CoC and CoD (Fig. 3). When the network is more rigid (CoA) the plateau is quickly achieved; on the other hand in the coatings with higher percentage of PVOH (CoC and CoD) the release process is influenced by the swelling process so the reaching of the plateau is delayed. In fact, when the PVOH-based active films are brought in contact with water, the polymer absorbs water and swells (Buonocore et al., 2003). This leads to an increase of the mesh size of the whole hybrid organic-inorganic network and to subsequent release of NAT into the food simulant liquid.

Furthermore, the maximal level of released NAT from each coating exhibited great differences: it was about 0.016 ± 0.001 mg/dm² for CoA, 0.032 ± 0.002 mg/dm² for CoB, 0.059 ± 0.001 mg/dm² for CoC and 0.105 ± 0.001 mg/dm² for CoD (Fig. 7). These results showed that the amount of released NAT increased with the O/I ratio parallel to the increased weight of the coatings, as discussed above.

Figure 8 shows a comparison between NAT entrapped and NAT released by the four coatings. It can be seen that the amount of released antimycotic is always a small percentage respect to that entrapped. This may suggest that the activity of NAT coatings could be exerted by direct contact rather than through a progressive release of the active substance to a food product. This can represent a great advantage since a very little amount migrates to food. Moreover, the liquid environment employed to test the release kinetic most probably leads to overestimate the result respect to the real amount that may migrate to a solid product as a cheese sample.

Our results can also be considered an indirect way to assess the stability of the coatings when placed in water: at higher content of PVOH the contact with water does not affect the integrity of the network avoiding its disintegration, demonstrating that CoD is the more stable.

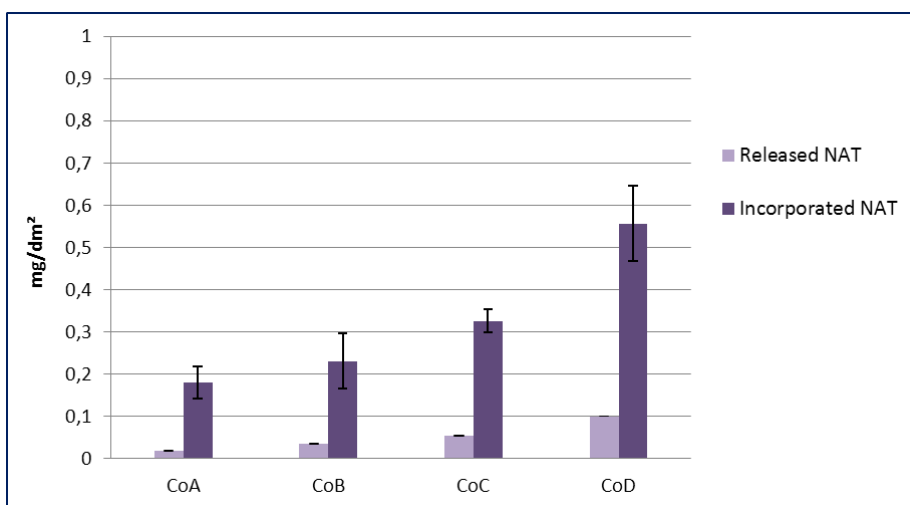


Fig. 8. Amount of released and incorporated NAT (mg/dm^2) into liquid food simulant for each coating.

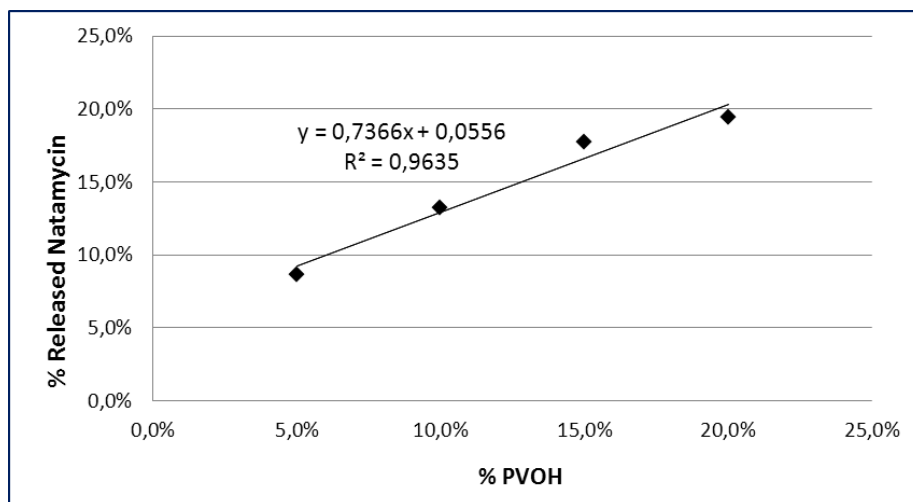


Fig. 9. Percentage of NAT released from each coating (in order, from the first point: CoA, CoB, CoC and CoD) as function of the percentage of PVOH.

In the Fig. 9 is reported the linear plot obtained by calculating the percentage of released NAT respect to the entrapped one. It can be seen that this value shows a positive correlation with the percentage of PVOH. Also this behavior is related to the above mentioned swelling process: the loose of network with extremely mobile chains, deriving from water contact, facilitated the loss of NAT.

2.4. Conclusions

In this study, four sol-gel active coatings on PLA films including NAT as an antimicrobial agent were prepared using different organic-inorganic ratio.

This technique allows production of novel food packaging materials in which it is possible to modulate the level of NAT incorporated in the films, since its amount has been found to increase during the deposition step with the increasing of PVOH percentage. At the same time the percentage of release of NAT increased, as assessed by the release tests carried out into food simulant liquid by HPLC-UV-VIS. The described release from the films was found to be initially controlled by a Fickian diffusion.

In all cases the amount of NAT detected in simulating liquid was lower than that allowed in the superficial part of the rind of cheese, i.e. 1 mg/dm², according to Directive 95/2/EC. Moreover, all the coatings protected the surface of commercial semi-soft cheese against the development of undesirable moulds growth, independent of O/I ratio. In particular, CoA coating showed excellent properties in terms of food conservation, acting probably by contact, or releasing the minimum amount of NAT sufficient at inhibiting the mould growth. In conclusion, the obtained results suggest that the sol-gel active coatings on polylactic acid films prepared in this study may be used as novel, controlled release food packaging materials. However, further studies are needed to measure their antimicrobial activities on selected microorganisms and on other real food surfaces.

2.5. References

Alfieri, I., Lorenzi, A., Montenero, A., Gnappi, G., and Fiori, F., 2010. Sol-gel silicon alkoxides–polyethylene glycol derived hybrids for drug delivery systems. *Journal of Applied Biomaterials and Biomechanics*, 8, 14–19.

Appendini, P., and Hotchkiss, J. H. (2002). Review of antimicrobial food packaging. *Innovative Food Science and Emerging Technologies*, 3, 113–126.

Bierhalz, A. C. K., da Silva, M. A., and Kieckbusch, T. G., 2012. Natamycin release from alginate/pectin films for food packaging applications. *Journal of Food Engineering*, 110, 18–25.

Bierhalz, A. C. K., da Silva, M. A., de Sousa, H. C., Braga, M. E. M., and Kieckbusch, T. G., 2013. Influence of natamycin loading methods on the physical characteristics of alginate active films. *The Journal of Supercritical Fluids*, 76, 74-82.

Buonocore, G. G., Del Nobile, M. A., Panizza, A., Corbo M. R., and Nicolais, L., 2003. A general approach to describe the antimicrobial agent release from highly swellable films intended for food packaging applications. *Journal of Controlled Release*, 90, 97–107.

Buonocore, G. G., Conte, A., Corbo, M. R., Sinigaglia, M., and Del Nobile, M. A., 2005. Mono- and multilayer active films containing lysozyme as antimicrobial agent. *Innovative Food Science and Emerging Technologies*, 6, 459 – 464.

Chen, G. Q., Lu, F. P., and Du, L. X., 2008. Natamycin production by *Streptomyces gilvosporeus* based on statistical optimization. *Journal Agricultural and Food Chemistry*, 56(13), 5057-5061.

Corradini, C., Alfieri, I., Cavazza, A., Lantano, C., Lorenzi, A., Zucchetto, N., and Montenero, A., 2013. Antimicrobial films containing lysozyme for active packaging obtained by sol–gel technique. *Journal of Food Engineering*, 119(3), 580–587.

de Oliveira, T. M., de Fátima Ferreira Soares, N., Pereira, R. M., and de Freitas Fraga, K., 2007. Development and Evaluation of Antimicrobial

Natamycin-incorporated Film in Gorgonzola Cheese Conservation. *Packaging technology and science*, 20, 147-153.

Delves-Broughton, J., Thomas, L.V., Doan, C.H., and Davidson, P.M., 2005. Natamycin. In: Davidson, P.M., Sofos, J. N., Branen, A.L.(Eds.), *Antimicrobials in Food*, CRC Press, Boca Raton, 275–289.

Directive 95/2/EC of the European Parliament and of the Council (1995) Annex III part C. On food additives other than colours and sweeteners. Off J Eur Communities 18.03.1995:L61.

Fajardo, P., Martins, J. T., Fucinos, C., Pastrana, L., Teixeira, J. A., and Vicente, A. A., 2010. Evaluation of a chitosan-edible film as carrier of natamycin to improve the storability of Saloio cheese. *Journal of Food Engineering*, 101, 349-356.

González, A., and Alvarez Igarzabal, C. I., 2013. Soy protein - Poly (lactic acid) bilayer films as biodegradable material for active food packaging. *Food Hydrocolloids*, 33, 289-296.

Guarino, C., Fuselli, F., La Mantia, A., and Longo, L., 2011. Development of an RP-HPLC method for the simultaneous determination of benzoic acid, sorbic acid, natamycin and lysozyme in hard and pasta filata cheeses. *Food Chemistry*, 127, 1294–1299.

Hanušova, K., Štastná, M., Votavová, L., Klaudivsová, K., Dobiáš, J., Voldrich, M., and Marek, M., 2010. Polymer films releasing nisin and/or natamycin from polyvinylidene chloride lacquer coating: Nisin and natamycin migration, efficiency in cheese packaging. *Journal of Food Engineering*, 99, 491–496.

Kallinteri, L.D., Kostoula, O. K., and Savvaidis, I. N., 2013. Efficacy of nisin and/or natamycin to improve the shelf-life of Galotyri cheese. *Food Microbiology*, 36, 176-181.

Koide, S., and Shi, J., 2007. Microbial and quality evaluation of green peppers stored in biodegradable film packaging. *Food Control*, 18, 1121–1125.

Mascheroni, E., Guillard, V., Nalin, F., Mora, and Piergiovanni L., 2010. Diffusivity of propolis compounds in Polylactic acid polymer for the development of anti-microbial packaging films. *Journal of Food Engineering*, 98, 294–301.

Minelli, M., De Angelis, M. G., Doghieri, F., Rocchetti, M., and Montenero, A., 2010. Barrier Properties of Organic–Inorganic Hybrid Coatings based on Polyvinyl Alcohol with improved water resistance. *Polymer engineering and science*, 50, 144-153.

Montenero, A., Passera, M., and Rocchetti, M., International Patent WO/2007/042993.

Quattara, B., Simard; R. E., Pierre, G., Bégin, A., and Holley, R. A., 2000. Inhibition of surface spoilage bacteria in processed meats by application of antimicrobial films prepared with chitosan. *International Journal of Food Microbiology*, 62, 139-148.

Reps, A., Drychowski, L. J., Tomasik, J., and Winiewska, K., 2002. Natamycin in ripening cheeses. *Pakistan Journal of Nutrition* 1 (5), 243-247.

Schottner, G., 2001. Hybrid Sol-Gel-Derived Polymers: Applications of Multifunctional Materials. *Chemistry. Material*, 13, 3422-3435.

Seydim, A.C., and Sarikus, G., 2006. Antimicrobial activity of whey protein based edible films incorporated with oregano, rosemary and garlic essential oils. *Food Research International*, 39, 639–644.

Sung, S. Y., Sin, L. T., Tee, T. T., Bee, S. T., Rahmat, A. R., Rahman, W.A.W.A., Tan, A. C., and Vikhraman, M., 2013. Antimicrobial agents for food packaging applications. *Trends in Food Science & Technology*, 33(2), 110-123.

Suppakul, P., Miltz, J., Sonneveld, K., and Bigger, S. W., 2003. Active packaging technologies with an emphasis on antimicrobial packaging and its application. *Journal of Food Science*;68(2), 408-420.

The Fitness for Purpose of Analytical Methods, 1998. A Laboratory Guide to Method Validation and Related Topics, Eurachem Guide, 1st English edition 1.0, LGC (Teddington) Ltd., <<http://www.eurachem.org/>>.

Ture, H., Eroglu, E., Ozen, B., Soyer, F., 2008. Antifungal activity of biopolymers containing natamycin and rosemary extract against *Aspergillus niger* and *Penicillium roquefortii*. *International Journal of Food Science and Technology*,43, 2026–2032.

Weng, Y. X., Jin, Y. J., Meng, Q. Y., Wang, L., Zhang, M., and Wang Y. Z., 2013. Biodegradation behavior of poly(butylene adipate-co-terephthalate) (PBAT), poly(lactic acid) (PLA), and their blend under soil conditions. *Polymer Testing*, 32, 918–926.

Zactiti, E. M., and Kieckbusch, T. G., 2009. Release of Potassium Sorbate from Active Films of Sodium Alginate Crosslinked with Calcium Chloride. *Packaging technology and science*, 22, 349-358.

Chapter 3

Effects of innovative/alternative steeping methods on antioxidant capacity, caffeine, catechins and gallic acid content of green, black and oolong tea infusions

3.1. Introduction

Tea represents one of the most popular and traditional beverages, consumed in China since a thousand years ago (Yang et al., 2007); today it represents the most consumed drink in the world after water (Cabrera et al., 2006). The market proposes several kinds of tea, originated from *Camellia sinensis* (earlier called *Thea sinensis*) of two subspecies: var. *sinensis* (China tea) and var. *assamica* (Assam tea) (Hilal and Engelhardt, 2007). According to the different ways of processing, especially the extent of fermentation, three basic types of tea are known: green tea (non-fermented), oolong tea (semi-fermented) and black tea (fully fermented) (Chaturvedula and Prakash, 2011). Black tea is the mostly consumed in Western countries, although great attention has been paid in recent years to the properties of green tea, mainly because of its higher antioxidant activity (McKay and Blumberg, 2002; Sharangi, 2009; Willson, 1999).

The traditional Chinese way of preparing teas is brewing tea leaves in hot water at a temperature depending on the tea type (70–80 °C for green tea, 80–90 °C for oolong, and 100 °C for black tea) during 20–40 s (Yang et al., 2007). The effect of infusion conditions on the bioactive compounds extraction in different type of tea has been studied (Araújo Ramalho et al., 2013; Chen et al., 2013; Rusak et al., 2008). Temperature of the water and infusion time have been found to be the most crucial parameters affecting polyphenol content and, as a result, the antioxidant capacity of green tea infusions. In particular, best extraction of antioxidant compounds from green tea was obtained at temperatures close to 80 °C, while 90 °C was recognized as a critical temperature at which polyphenols are destroyed. On the other hand,

agitation and dosage form have not been found to have an important influence (Samaniego-Sánchez, et al. 2011).

In recent times, cold water (4°C or room temperature) steeping is a new popular way for tea infusion in Taiwan, especially in summer time. Lin et al., (2008) indicated that the cold water steeped tea contains lower amount of caffeine, lower bitter taste and higher aroma, and would not influence sleep comparatively. For its preparation, the tea leaves/water ratio is similar to that of the traditional Chinese ceremonial tea making; tea leaves are steeped in 25 °C water at least for 2 h, or at 4 °C over 4 h. Yang et al. (2007) reported that the infusion rates of caffeine, catechins and gallic acid in cold water infuse were lower compared to hot water, and increased with increasing time of infusion. Similarly, Venditti et al. (2010) investigated how antioxidant activity was influenced by different preparation modality, in particular in hot or room-temperature water steeping. Their results contributed to further knowledge on how the potential health benefits of this popular beverage may be maximised by the different methods of preparation.

However, even if cold steeping could be a promising technology, it presents the great drawback represented by the long infusion times required. In order to overcome this difficulty, a potential modification of cold steeping method has been developed, and involves an infusion step with hot water, immediately followed by rapid cooling by ice addition. This process would also avoid the slow cooling process of the infuses, that was found to be responsible for changes in the contents of functional compounds (Yang et al., 2007). The effects of cold water steeping, as alternative condition, on functional compounds and infusion organoleptic quality were not yet investigated and deserve

more attention considering the global tea utilization and the advertised beneficial effects of its consumption on human health.

In this paper, we studied the effects of three different steeping methods on three tea types (black, green and oolong). The preparation methodologies examined were developed by a panel of experienced tea tasters, and involved: hot water, cold water, and hot water followed by ice addition. Antioxidant activity (determined by FRAP and total phenolic content evaluation), caffeine, theobromine, theophylline, catechins and gallic acid content were studied.

3.2. Materials and Methods

3.2.1. Reagents and chemicals

Gallic acid (GA), ascorbic acid, theobromine, theophylline, caffeine, (-)-epicatechin (EC), (-)-epigallocatechin gallate (EGCG), 2,4,6-Tripyridyl-s-triazine (TPTZ), glacial acetic acid, methanol (MeOH), acetonitrile (ACN), Folin Ciocalteu's phenol reagent and 2,2-difenil-1-picrilhydrazyl (DPPH) were purchased from Sigma–Aldrich Chemical Co. (St. Louis, MO, USA). Sodium acetate and ferric chloride were obtained from Carlo Erba Reagents (Milano, Italy). Phosphoric acid was supplied by J.T. Baker (Milano, Italy) and sodium carbonate by Across Organic Sigma–Aldrich Chemical Co. (Milano, Italy). Deionized water (< 18 MΩ cm resistivity) was obtained from a Milli-Q Element water purification system (Millipore, Bedford, MA, USA), while for preparation of teas, bottled mineral water was purchased from local retail (80.5 of dry residue at 180°C (mg/l), 124 μS/cm of conductivity at 25°C, and 5.9 °F hardness).

3.2.2. Teas and preparation of infusions

Three kinds of teas (Sencha Needle unfermented green, Tung Ting semi-fermented oolong and Orange Pekoe Flowery fully-fermented black) donated by “Ferri dal 1905” (Castel Goffredo, Mantova, Italy) were employed. The leaf size of green and black teas was about 1.5 mm while the leaf oolong tea was rolled and presented a diameter of about 3 mm. Estimated total surface available for mass diffusion of tea samples was 104.4, 44.8, and 16.8 mm² for oolong, green and black tea, respectively. Steeping methods were tuned by a panel of experienced tea tasters employed in the factory, and are reported in Table 1. The time and temperature of infusion were optimised for each type of tea. For extraction with hot water (named “hot”), each tea sample (12 g) was placed into a 1 L flask adding 1 L of water previously brought to specific temperature for specific time (see Table 1). Cold preparation of tea (named “cold”) was prepared by infusion at refrigeration temperature (4 °C ± 1) along 12 hours. Ice tea infusions (named “hot+ice”) were prepared by placing 30 g of tea in 660 mL of water at 80°C and, after the required time of infusion, the addition of 400 g of ice, after removal of leaves. All beverages were prepared in triplicate and filtered through a 0.45 mm nylon filter before analysis.

Table 1. Schematic description of the unconventional infusion preparations.

Tea	Extraction	Leaves (g/L)	Temperature (°C)	Time (min)	Water (L)	Ice (kg)*
Green	Hot	12	75	4	1	-
	Cold	8	4	720	1	-
	Hot+Ice	30	80	5	0.66	0.4
Oolong	Hot	12	85	4	1	-
	Cold	7	4	720	1	-
	Hot+Ice	30	80	4	0.66	0.4
Black	Hot	12	90	3	1	-
	Cold	7	4	720	1	-
	Hot+Ice	30	80	3	0.66	0.4

*added after infusion

3.2.3. High-performance liquid chromatography (HPLC)

An Agilent Technologies 1200 series liquid chromatograph system comprising pump, auto-sampler, thermostatted column compartment, and diode array detector was carried out. Separation was achieved on Kinetex, C18 column (100 mm x 2.1 mm ID), with particle size 2.6 μ . Analytical separation was optimised by modifying the method proposed by Wang et al. (Wang et al., 2000). The initial composition of the mobile phase was consisted of 85% solvent A water containing 0.1% (v/v) orthophosphoric acid) and 15% of solvent B (MeOH).

Solvent B was then increased linearly to 27% at 16 minutes. The gradient returned to 15% B in 1 min, standing at 15% for others 13 minutes as post-time at the flow rate of 0.2 ml/min. The column was thermostated at 30°C ($\pm 1^\circ\text{C}$) and the injected volume was 20 μl . Monitoring wavelengths were set at 210 nm and 280 nm.

For the quantification of the analytes, studies on linearity, precision, selectivity, and recovery were performed, according to Eurachem guidelines as reported in the Chapter 1 (Section 1.2.6.).

Linearity was established in the range of concentration between 0.05 and 100 mgL^{-1} for gallic acid and caffeine, 0.05-50 mgL^{-1} for teobromine, 0.05-25 mgL^{-1} for teofilline, 0.5-25 mgL^{-1} for epicatechin and 0.5-100 mgL^{-1} for epigallocatechin gallate, diluting the standard solution. Five equispaced concentration levels were chosen and three replicated injections were performed at each level. The homoscedasticity test was run and the goodness of fit of the calibration curve was assessed applying Mandel's fitting test. A t-test was carried out to verify the significance of the intercept (confidence level 95%). Precision was calculated in terms of inter-day and intra-day repeatability both of area and retention times as R.S.D. % at two concentration levels for analysis.

Intra-day repeatability was calculated on peak areas and on retention times using five determinations at two concentration levels in triplicate. Inter-day repeatability was calculated performing the same analyses in two different days.

3.2.4. Total phenolic content (TPC)

Total phenol content of the different tea samples was determined according to the Folin–Ciocalteu procedure as described by Jayasekera, et al., (2011), with some modification. Briefly, to an aliquot of 1 mL of each tea, 4 mL of 7.5% sodium carbonate solution and 5 mL Folin–Ciocalteu phenol reagent (10%) were added to reach a final volume of 10 mL. The mixture was allowed to react for 60 min at room temperature in the dark. The absorbance of the reaction mixture was read at 750 nm. Calibration was achieved with an aqueous gallic acid solution (25–300 µg/mL). Total phenol values were expressed as gallic acid equivalents (GAE) based on the calibration curve. The assay was carried out in triplicate for duplicate extractions giving six observations for each sample. Values given for each sample are means of six observations.

3.2.5. Determination of ferric reducing antioxidant power (FRAP)

The ferric reducing/antioxidant power (FRAP) assay was carried out according to Benzie and Strain (1996). This assay measures the change in absorbance at 593 nm owing to the formation of a blue colored FeII-tripyridyltriazine compound from the colorless oxidized FeIII form by the action of electron donating antioxidants (Benzie et al., 1999). The working FRAP was prepared by mixing acetate buffer 300 mM, pH 3.6, TPTZ 10 mM and FeCl₃ · 6H₂O (20 mM water solution) at a ratio of 10:1:1. Briefly, to a volume of 200 mL of tea infusions, 380 µL of working FRAP previously warmed to 37°C for 10 minutes was added.

Immediately and after 4 min the absorbance of blue coloration was measured at 593 nm against a blank sample.

3.2.6. Statistical analysis

Means and standard deviations (SD) of data were calculated with SPSS (Version 20.0) statistical software. SPSS was used to perform one-way analysis of variance (ANOVA) and the least significant difference (LSD) test at a 95 % confidence level ($p < 0.05$) and further used to identify differences among samples.

3.3. Results and discussion

3.3.1 High-performance liquid chromatography (HPLC)

The first step of the work was related to the optimisation of a chromatographic method for the separation of the different molecules object of the study. The analytes of interest were xanthines (caffeine, theophylline and theobromine), catechins (epicatechin, and epigallocatechin gallate) and gallic acid. All analytes were well separated in about 14 minutes (Figure 1) and contents are reported in Table 2, where it can be seen that in most cases significant differences were observed between the different steeping methods. Data are reported as mg/g of tea leaves, in order to show the effectiveness of extraction notwithstanding the differences in the leaves:water ratio employed by the three infusion methods.

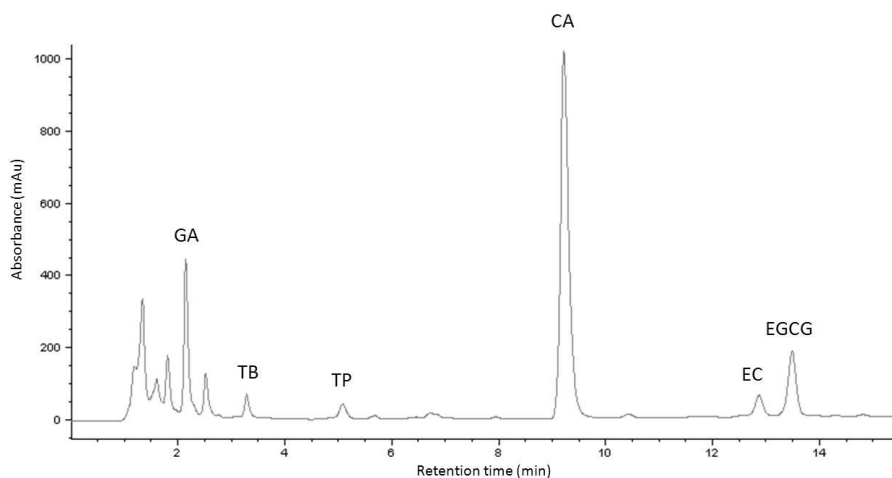


Fig. 1. HPLC chromatogram of a cold infuse of green tea recorded at 210 nm. GA - gallic acid TB - theobromine, TP – theophylline, CA – caffeine, EC – epicatechin, EGCG – epigallocatechin gallate.

EGCG has been found to be the most predominant catechin in all beverages confirming previous literature data (Goto et al., 1996, Friedman et al., 2006, Wang et al., 2000). Among xanthines, caffeine (discussed below) showed the highest content, followed by theobromine and then, theophylline; obtained values were in accord to ranges reported in literature for tea infuses (Friedman et al., 2006). Gallic acid was detected in significant amounts, ranging from 1.05 to 5.13 mg/g, sensibly higher than that previously reported (Wang et al., 2000).

In particular, for green and black tea, it can be noticed that hot+ice infusion, characterised by a higher temperature and short time of contact with water, allowed extracting the highest amount of all

analytes, except TP whose amount was constant in all infuses (Table 2).

Table 2. Analytical results of tea samples *

Tea	Extraction	FRAP	TPC	GA	EC	EGCG	TP	TB
Green	Hot	1463.1±129.7a	13.5±0.1c	3.46±0.03c	1.36±0.06b	4.09±0.12b	0.20±0.00a	0.63±0.01b
	Cold	1653.5±147.1a	19.7±0.1a	3.93±0.03b	n.d.	4.13±0.10b	0.19±0.01a	0.65±0.03b
	Hot+Ice	1432.6±80.8a	14.2±0.0b	5.13±0.06a	1.61±0.05a	7.36±0.02a	0.19±0.00a	1.22±0.03a
Oolong	Hot	325.4 ± 64.9b	12.8±0.2c	1.05±0.01c	0.23±0.05a	0.62±0.01c	0.06±0.01b	0.25±0.01b
	Cold	1278.5 ± 81.1a	21.0±0.1a	2.94±0.02a	n.d.	2.45±0.01a	0.24±0.01a	0.43±0.01a
	Hot+Ice	1183.5±124.3a	14.1±0.2b	2.12±0.02b	0.11±0.02b	1.17±0.07b	0.06±0.00b	0.25±0.00b
Black	Hot	1111.8±139.2b	14.2±0.1b	3.62±0.15b	n.d.	0.43±0.01c	0.09±0.00a	1.29±0.01b
	Cold	1218.8 ± 38.0b	20.4±0.1a	4.11±0.14a	n.d.	0.60±0.01b	0.10±0.01a	1.15±0.00c
	Hot+Ice	1629.0±189.6a	14.8±0.2b	4.07±0.15a	0.03± 0.00	0.76±0.03a	0.11±0.01a	1.62±0.06a

*Data (mean ± standard deviation) are expressed as mg/g of tea leaves

Abbreviations: gallic acid (GA), (-)-epigallocatechin (EGC), (-)-epicatechin (EC),

(-)-epigallocatechin gallate (EGCG), Theophylline (TP) and Theobromine (TB)

n.d. < LOQ

^{a,b,c} Same letters within each column do not significantly differ (n=5; p<0.05).

Extraction of compounds clearly depends on both temperature and time of infusion. Thus, temperature seems to represent the most influential parameter affecting the migration of substances into water. This result is in agreement with Yang et al. (2007) who reported a much lower infusion rate of gallic acid from green tea bags with cold water steeping when compared to that prepared with hot one. On the contrary, Damiani et al. (2013) found, for white tea, higher amounts of catechins and gallic acid in cold infuses than in hot ones.

For both green and black tea, cold method allowed, for some compounds, the extraction of slightly higher amounts than hot method, showing that the longer time of contact in cold method ensures the migration of a relevant amount of some compounds even at low temperature. It can also be hypothesized that higher amounts of analytes are extracted during long time, but then, they are destroyed by oxidation or other side reactions such as polymerization phenomena occurring along 12 hours (Samaniego-Sanchez et al., 2011; Kim et al 2007). Another explanation might be that such phenomena could also occur in the hot teas after the infusion step, during the slow process of cooling at room temperature, while hot+ice infuses reach quickly a low temperature because of the ice addition, consequently keeping higher amount of active compounds. Oxidative degradation of EGCG has been previously reported to occur during storage of infuses (Yang, 2007) since this compound is not stable at high temperature; accordingly, in the present paper, its amount was found to be definitely higher in both “hot+ice” and cold infuses compared to hot ones (Table 2). In the same way, Kim et al (2007) observed a decreasing trend in catechins at high temperature, suggesting that epimerization or oxidation could take place. Moreover it can be noticed that EC was not found in cold infuse.

Different results were obtained from the analysis of oolong tea: in this case the highest values for all analytes were found with cold extraction. This apparently unexpected behaviour can be explained by considering the shape and dimension of the employed leaves: the leaf of oolong tea has a diameter (about 3 mm) higher than those of other teas, and its total surface available for mass diffusion (104.4 mm²) is definitely

bigger (Astill et al., 2001). The leaves are rolled, and this shape can lead to a difficulty in the extraction kinetics, slowing the migration process. Therefore, longer time of contact with water, although at low temperature, allowed the migration of the active compounds. As for the comparison between hot and hot+ice methods, it can be seen that, similarly to what observed in green tea, a double amount of gallic acid and ECGC was recorded in the latter extract respect to the former, while the opposite happened for EC.

Finally, in black tea, smaller differences between the three steeping procedures were observed, with slight higher values for hot+ice method than other infuses, and lower values for hot extraction. Since hot extraction was performed at 90 °C, the highest temperature employed in all experiments, our results confirm previous findings reporting that a too high temperature can lead to the destruction of the extracted compounds (Samaniego-Sanchez et al., 2011)

As reported above, EC was not detected in cold infuses, regardless of variety.

In conclusion, data about catechins content in different teas are in agreement with Yang et al., 2007 and also, Kim et al., 2007 who observed that the amounts of total catechins were ordered according to the fermentation processes as follows: non-fermented (green tea) > partially fermented (oolong tea) > fully fermented (black tea).

Data about caffeine contents, expressed as mg/g of dry leaves are reported in Figure 2. Measured caffeine contents were in the ranges previously reported for all the considered tea varieties (Cabrera, et al., 2003). Green tea presented higher values compared to both black and oolong ones, as previously reported by Yang et al., (2007). Caffeine extraction directly depends on infusion temperature with a higher mass

transfer rate with increasing water temperature (Perva-Uzunalić et al., 2006). For green tea, the highest value was recorded for hot+ice extraction, similarly to black tea where the amounts of hot and hot+ice extraction were similar. On the contrary, for oolong tea, cold method gave the highest value. Thus, it can be concluded that for green and black tea, the leaves dimension represents the limiting factor for mass transfer, and water temperature played an important role in caffeine extraction. Besides, in oolong tea the great surface/volume ratio allowed an efficient extraction also at low temperature, as demonstrated by the very high concentration of caffeine in cold extraction (Figure 2) due to the longer infusion time.

Finally, since caffeine is an important psychoactive drug, whose intake is of great interest in diet, and whose consumption should be taken under control, we took into account the amount of caffeine occurring in the beverages. Therefore, caffeine content was calculated as amount contained in a cup (200 mL) of final drink (Price et al., 1998), considering the differences between the leaves:water ratio employed by the three infusion methods and data are reported in Figure 2 panel b. In this way, the real intake for a tea habitual consumer can be evaluated notwithstanding the different procedures of preparation. For all teas, the hot+ice method gave the highest value of caffeine content, because of the greater leaves:water ratio used for this preparation (Table 1), obviously, this parameter directly influenced caffeine extraction (Perva-Uzunalić et al., 2006). Great differences between hot+ice and other steeping methods were observed for green and black teas due to their low surface/volume value, as stated above. As expected, hot method gave higher amount of caffeine than cold one

because of the higher leaves:water ratio employed, but also since high temperature favoured the extraction process.

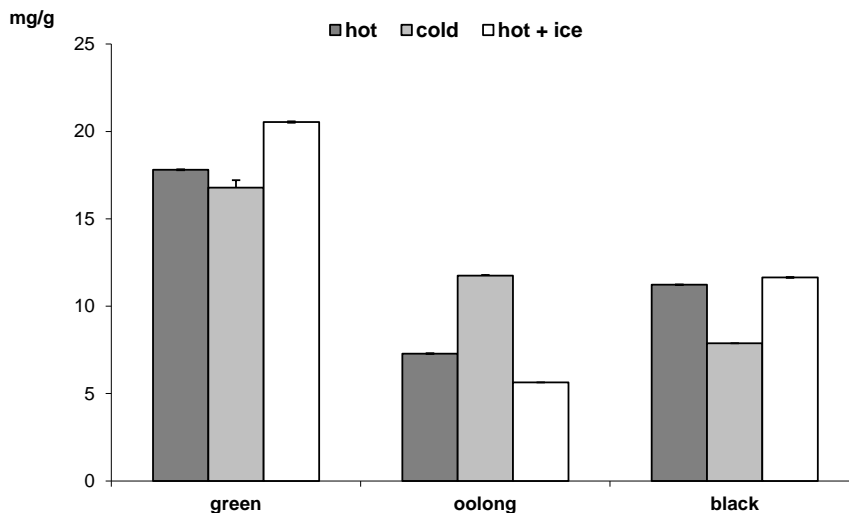


Fig. 2. Caffeine content expressed as mg/g of tea leaves.

3.3.2 Total phenolic content

The total phenolic content was evaluated by the Folin-Ciocolteau method, giving an estimation of the total reducing power of the extract, since this assay is also sensible to all compounds with reducing properties. The results of this assay are of great interest, because the amount of phenolics is generally connected to beneficial health effects of food, and in particular of tea, especially green one, that is usually considered a major source of antioxidants.

No great differences were observed between the behaviour of the different infusion methods for the three tea types, as data were found to follow a similar trend (Table 2). For all teas, cold infusion gave the

highest phenolic content, followed by hot+ice and then hot method, in accordance to the recent data from Damiani et al. (2013) on white tea, but in contrast with Venditti et al. (2010) which reported a general higher TPC in hot black, oolong and green teas than in cold ones. Two possible reasons could explain this behaviour: the longer time of extraction determined the migration of a higher amount of active compounds (as also reported by Yang et al., 2007) and/or the low temperature that protected these molecules from degradation.

To understand which could be the predominant variable affecting the obtained value, among time and temperature, we took into account the data from the other extracts. It seems that time is the predominant effect in increasing the extraction process, while high temperature, as reported above, has been found to lead to destruction of the molecules causing oxidation, epimerization and polymerization phenomena. Therefore, we can assume that the rapid cooling in the hot+ice method limited those effects, exerting a protective effect on the molecules that were not subjected to a long exposition to high temperature.

The total phenolic content was evaluated by the Folin-Ciocolteau method, giving an estimation of the total reducing power of the extract, since this assay is also sensible to all compounds with reducing properties. The results of this assay are of great interest, because the amount of phenolics is generally connected to beneficial health effects of food, and in particular of tea, especially green one, that is usually considered a major source of antioxidants.

No great differences were observed between the behaviour of the different infusion methods for the three tea types, as data were found to follow a similar trend (Table 2). In all tea types, cold infusion gave the

highest phenolic content, followed by hot+ice, and then by hot extraction. These findings are in accordance to the recent data from Damiani et al. (2013) on white tea, but in contrast with Venditti et al. (2010) which reported a general higher TPC in hot black, oolong and green teas than in cold ones. Two possible reasons could explain this behaviour: the longer time of extraction determined the migration of a higher amount of active compounds (as also reported by Yang et al., 2007) and/or the low temperature that protected these molecules from degradation.

To understand which could be the predominant variable affecting the obtained value, among time and temperature, we took into account the data from the other extracts. It seems that time is the predominant effect in increasing the extraction process, while high temperature, as reported above, has been found to lead to destruction of the molecules causing oxidation, epimerization and polymerization phenomena. In fact high temperature does not affect molecules stability since the value recorded after hot extraction was higher than that of hot+ice extraction. Therefore, it appears that higher temperature helps the migration without destroying the phenolic molecules (while the opposite behaviour was observed for the FRAP value, see below).

3.3.3. *FRAP value*

From the comparison of the data related to antioxidant power of the three tea types (Table 2) it can be seen that generally, very high values were recorded for green tea. For this tea, no differences between extraction methods were observed. This confirms that green tea is richer of antioxidant compounds, according to literature data (von

Gadow et al., 1997), and suggests that the compounds responsible for this activity are also stable at high temperature.

On the contrary, the lowest values were recorded for oolong tea, suggesting that this tea may contain less active compounds. Besides, since cold and hot+ice extractions gave higher values than hot infusion, we may assume that the compounds reacting in FRAP test for oolong tea are quite sensible to high temperature (Yang 2007; Damiani et al. (2013). In addition, we can hypothesize that the very high exchanging surface at the longer time of extraction in cold method, determined the extraction of a higher amount of active compounds. At the same time, the low temperature protected the antioxidant molecules from degradation.

A similar behaviour has been noticed for black tea: hot+ice infusion gave the highest value, while no significant differences between the other extracts were observed.

The high variability found between the behaviour of the three tea types suggests that the pattern of the compounds responsible for the antioxidant activity is probably different and/or a different kinetic of migration of the active molecules from the leaves to the solution occurred.

Nevertheless, it is very important to bear in mind that it is not correct to compare these activities among the teas because the tea leaves composition and the infusion concentration depends on many parameters such as cultivar type, growing environment (country, altitude, soil, climate), plucking practices (age of leaf) and manufacturing conditions (Astill et al., 2011).

3.4. Conclusions

The present study compared the effects of the classical hot extraction with alternative steeping methods (cold water and hot infusion followed by ice addition) on chemical compounds extraction, antioxidant activity, total phenolic content, of green, oolong and black teas.

Notwithstanding tea variety, ice addition after hot infusion gave the lowest extraction of caffeine per g of dry leaves and total phenols, as well as the lowest FRAP value, confirming that rapid cooling of infusion actually. On the contrary, cold extraction allowed obtaining high antioxidant activity, total phenolics and gallic acid content, confirming the raising popularity of this technique and literature data.

In conclusion, this study adds new information on how different drinking habits in specific countries and cultures as well as non-conventional preparation methods influence extraction of active compounds from tea leaves. The obtained results contribute to investigate new ways for maximising the potential health benefits of tea by means of different methods of preparation.

3.5. References

Araújo Ramalho, S., Nigam N., Barbosa Oliveira, G., Alves de Oliveira, P., Matos Silva, T. O., Geovânia Passos dos Santos, A., and Narendra, N., 2013. Effect of infusion time on phenolic compounds and caffeine content in black tea. *Food Research International*, 51(1), 155-161.

Astill, C., Birch, M.R., Dacombe, C., Humphrey, P.G., and Martin, P.T., 2001. Factors affecting the caffeine and polyphenol contents of black and

green tea infusions. *Journal of Agricultural and Food Chemistry*, 49, 5340–5347.

Benzie, I.F.F. and Strain J.J., 1996. The ferric reducing ability of plasma (FRAP) as a measure of “antioxidant power”: The FRAP Assay. *Analytical biochemistry*, 239, 70–76.

Benzie, I.F.F., Chung W.Y., and Strain J.J., 1999. “Antioxidant” (reducing) efficiency of ascorbate in plasma is not affected by concentration. *The Journal of Nutritional Biochemistry*, 10, 146-150.

Cabrera, C., Giménez, R., and Lòpez, M. C., 2003. Determination of Tea Components with Antioxidant Activity. *Journal of Agricultural and Food Chemistry*, 51,4427-4435.

Cabrera, C., Artacho, R., and Giménez, R., 2006. Beneficial effects of green tea—A review. *Journal of the American College of Nutrition*, 25, 79–99.

Chaturvedula, V.S.P., and Prakash, I., 2011. The aroma, taste, color and bioactive constituents of tea. *Journal of Medicinal Plants Research*, 5, 2110-2124.

Chen, Y.J., Kuo, P. C., Yang, M. L., Li, F. Y., and Tzen, J. T.C., 2013. Effects of baking and aging on the changes of phenolic and volatile compounds in the preparation of old Tieguanyin oolong teas. *Food Research International*, 53 (2), 732-743.

Damiani, E., Bacchetti, T., Padella, L., Tiano, L., and Carloni, P., 2013. Antioxidant activity of different white teas: Comparison of hot and cold tea infusions. *Journal of Food Composition and Analysis*, in press.

Eurachem working group (1998). The fitness for purpose of analytical methods. In *Eurachem guide* (1st ed. *Using validation data to design QC*, pp. 35–37). Middlesex, UK: Teddington.

Friedman, M., 2006. Overview of antibacterial, antitoxin, antiviral, and antifungal activities of tea flavonoids and teas. *Molecular Nutrition & Food Research*, 51, 116 – 134.

Goto, T., Yoshida, Y., Kiso, M., and Nagashima, H., 1996. Simultaneous analysis of individual catechins and caffeine in green tea. *Journal of Chromatography A*, 749, 295–299.

Hilal, Y., and Engelhardt, U., 2007. Characterisation of white tea– Comparison to green and black tea. *Journal für Verbraucherschutz und Lebensmittelsicherheit*, 2, 414-421.

Jayasekera, S., Molan A.L., Garg M., and Moughan, P.J., 2011. Variation in antioxidant potential and total polyphenol content of fresh and fully-fermented Sri Lankan tea. *Food Chemistry*, 125, 536-541.

Kim, E.S., Liang, Y.R., Jin, J., Sun, Q.F., Lu, J.L., Du, Y.Y., and Lin, C., 2007. Impact of heating on chemical compositions of green tea liquor. *Food Chemistry*, 103, 1263-1267.

Lin, S.D., Liu, E.H., and Mau, J.L., 2008. Effect of different brewing methods on antioxidant properties of steaming green tea. *LWT-Food Science and Technology*, 41, 1616-1623.

McKay, D.L., and Blumberg, J.B. (2002). The role of tea in human health: An update. *Journal of the American College of Nutrition*, 21, 1–13.

Perva-Uzunalić, A., Škerget, M., Knez, Ž., Weinreich, B., Otto, F., and Grüner, S., 2006. Extraction of active ingredients from green tea (*Camellia sinensis*): extraction efficiency of major catechins and caffeine. *Food Chemistry*, 96, 597-605.

Rusak, G., Komes, D., Likić, S., Horžić, D., and Kovač, M., 2008. Phenolic content and antioxidative capacity of green and white tea extracts depending

on extraction conditions and the solvent used. *Food Chemistry*, *110*, 852–858.

Samaniego-Sánchez, C., Inurreta-Salinas, Y., Quesada-Granados, J.J., Blanca-Herrera, R., Villalón-Mir, M., López-García de la Serrana, H., and López Martínez, M.C., 2011. The influence of domestic culinary processes on the Trolox Equivalent Antioxidant Capacity of green tea infusions. *Journal of Food Composition and Analysis*, *24*, 79-86.

Sharangi A.B., 2009. Medicinal and therapeutic potentialities of tea (*Camellia sinensis* L.) – A review. *Food Research International*, *42*, 529–535.

Venditti, E., Bacchetti, T., Tiano, L., Carloni, P., Greci, L., and Damiani, E., 2010. Hot vs. cold water steeping of different teas: Do they affect antioxidant activity?. *Food Chemistry*, *119*, 1597-1604.

von Gadow, A., Joubert, E., and Hansmann, C.F., 1997. Comparison of the antioxidant activity of rooibos tea (*Aspalathus linearis*) with green, oolong and black tea. *Food Chemistry*, *60*, 73-77.

Yang, D.J., Lucy S.H., and Jau-Tien L., 2007. Effects of different steeping methods and storage on caffeine, catechins and gallic acid in bag tea infusions. *Journal of Chromatography A*, *1156*, 312-320.

Wang, H., Helliwell, K., and You, X., 2000. Isocratic elution system for the determination of catechins, caffeine and gallic acid in green tea using HPLC. *Food chemistry*, *68* (1), 115-121.

Willson, K. C. (1999). *Coffee, Cocoa and Tea*. (1st ed.) New York: CABI Publishing.

Chapter 4

Development of new analytical methods for the determination of potentially toxic substances released from food contact materials

4.1. Introduction

As previously discussed, besides the positive migration of active substances, undesired chemical components such as plasticizers, monomers or mineral oils, may migrate from packaging into food, affecting the quality and mainly the safety. Furthermore some chemical compounds, known as non-intentionally added substances (NIAS), may be present in the packaging. In fact raw materials and additives used in the production of Food Contact Materials often contain impurities. Major impurities are generally known by the producer, but minor impurities may remain unknown as well as various contaminants from recycling processes and both their detection and identification can be complicate. In this chapter the development of new analytical method for the determination of potentially toxic substances released from polycarbonate is reported.

4.1.1. Polycarbonate

Polycarbonate (PC) is a thermoplastic polymer that finds many industrial applications, due to good properties like low weight, high toughness, strength and transparency (Xin-Gui and Mei-Rong, 1999). Bisphenol A (BPA) is widely used as the monomer for the production of food contact polycarbonate products such as food containers, baby bottles, toys (Ballesteros-Gomez et al., 2009; Piringer and Baner, 2008). However the use of BPA in plastic infant feeding bottles has been banned due to endocrine and reproductive effects on the human body, and effects on the immune system and the neurodevelopment,

especially considerable to infants (Commission Directive 2011/8/EC, 2011). Furthermore BPA-PC is particularly sensitive to the influence of UV-light, humidity and oxygen (Zweifel, 1998). Photo-Fries rearrangement and photo-oxidation, reported in Figure 1 and Figure 2 respectively, have been shown to be responsible for its discolouration and yellowing (Factor and Chu, 1980; Factor et al., 1987; Diepens and Gijsman, 2007; Pickett, 2011) depending on the irradiation wavelengths. In fact photo-Fries rearrangement reactions are observed at shorter wavelengths (<300 nm) while photo-oxidation mechanisms are more relevant when light of longer wavelengths is involved (>340 nm) (Rivaton et al., 1983). Whether these reaction pathways act independently (Factor and Chu, 1980; Rivaton, 1995; Pickett, 2000) or the photo-Fries products may act as promoters for photo-oxidation (Diepens and Gijsman, 2007) is still object of studies.

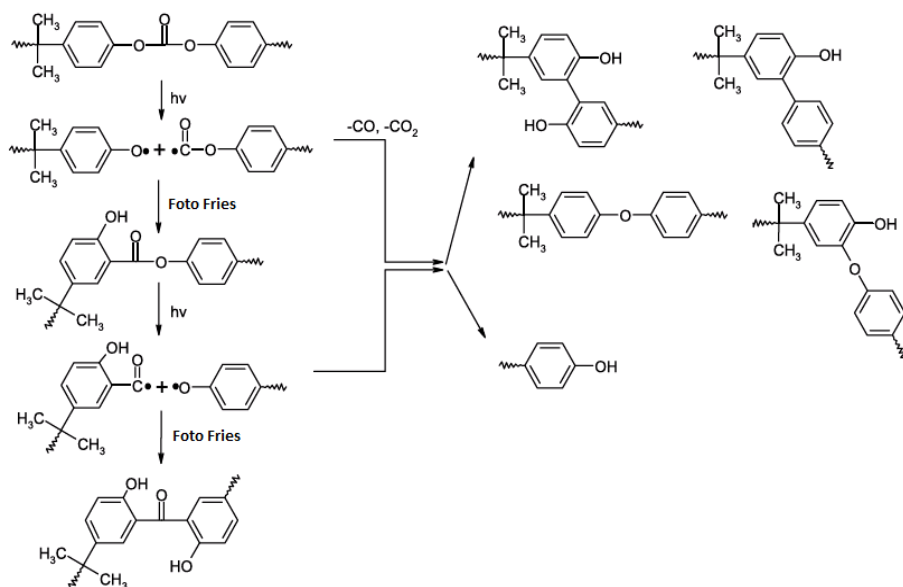


Fig. 1. Photo-Fries rearrangement via the radical process (Rivaton, 1995)

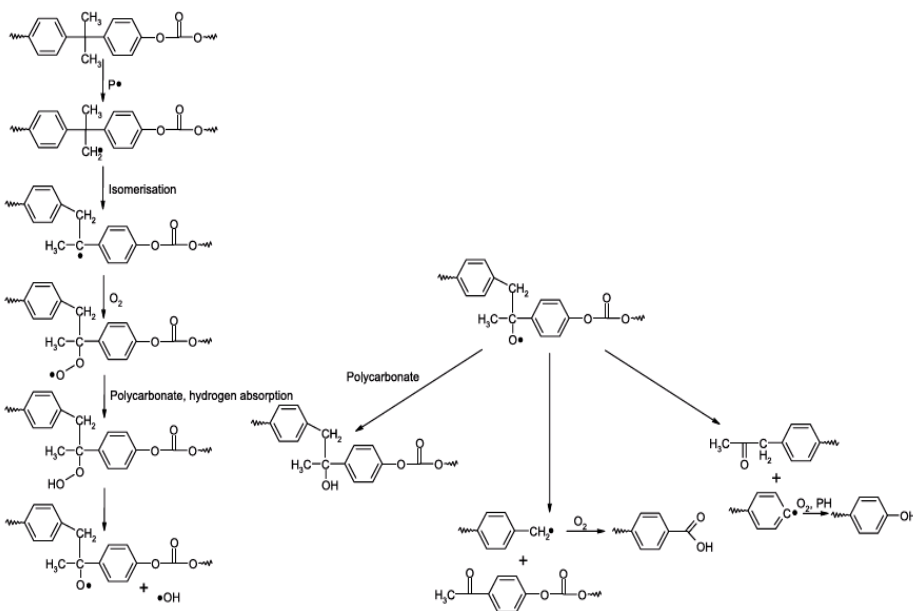


Fig. 2. Photo-oxidation of BPA-PC (Rivaton, 1995)

The most common additives, used to increase the lifetime and to improve physical properties of PC, (Galotto et al., 2001) are UV-absorbers (Diepens and Gijsman, 2010), primary and secondary antioxidants, and plasticizers (Nerìn et al., 2003).

These additives, as well as BPA and its degradation products, can be transferred to food by migration processes (Alin and Hakkarainen, 2012). To control eventual food contamination, high-performance liquid chromatography (HPLC) coupled to electrochemical (Rykowska and Wasiak, 2006), ultraviolet (Nerìn et al., 2003) fluorescence detection (Cabado et al., 2008), as well as immunochemical methods (Ballesteros-Gomez et al., 2009) are used for their identification. Mass spectrometry (MS) represents one the most frequently employed

technique for direct analysis of polymer samples (Schnoller et al., 2009), as well as for polymer additives after extraction (Alin and Hakkarainen, 2012; Cacho et al., 2014; Klampfl, 2013).

The present work is focused on the development of a new analytical method based on the combination of GC coupled to flame-ionization detector (FID) and to Fourier Transform Infrared Spectroscopy (FTIR), for the identification of polycarbonate compounds and additives which could migrate into food. The most important advantages of the FTIR are the possibility of distinguish similar molecules such as isomers and to obtain the unique infrared spectrum of each chemical substance rather than the fragments by MS (Cai et al., 2006).

Since the photo-degradation of PC is a surface phenomenon extending only about 25 μm into the exposed surface (Nagai et al., 2003), experiments in climatic chamber on polycarbonate tableware stored at room temperature and light exposure were examined by FT-IR in ATR mode.

The samples were also rinsed with alkaline detergent and sparkling aid and analyzed by FT-IR in ATR mode, in order to evaluate the possible residuals occurring after common washing procedure. As reported in literature, the release of BPA increases by increasing the pH of the washing solution (Hoekstra and Simonuau, 2013).

4.2. Materials and methods

4.2.1. Chemicals, Reagents and Materials

Water (LC-MS grade), ethanol (absolute), acetone (for HPLC, $\geq 99.9\%$), hexane (for HPLC, $\geq 95\%$), chloroform (100% HPLC grade), methanol (99.9% LC-MS grade), butylated hydroxyanisole (BHA,

98,5% purity); 2,6-Di-*tert*-butyl-4-methylphenol (BHT, $\geq 99\%$ purity); 9,9-DIMETILXANTENE (96% purity); 4-OCTYL-PHENOL (99% purity); 4-NONYL-PHENOL ($\geq 99\%$ purity); 2-Hydroxy-4-methoxybenzophenone (CYASORB UV9, 98% purity); Bisphenol A (99% purity); 2,2'-Methylenebis(6-*tert*-butyl-4-methylphenol) CYANOX 2246, ≥ 98.5 purity); 3-*tert*-Butyl-2-Hydroxy-5-Methylphenyl Sulfide IRGANOX 1081; 2-(2H-benzotriazol-2-yl)-4,6-ditertpentylphenol (TINUVIN 328, 98% purity); 4-4'-Butylidenebis(6-*tert*-butyl-*m*-cresol) (ANTYOXIDANT YS 40); 2-Hydroxy-4-(octyloxy)benzophenone (CHIMASSORB 81, 98% purity) were obtained from Sigma-Aldrich (Gallarate, Italy). Polycarbonate tableware were purchased from local supermarket and detergent Polypro and Sparkling aid: Suma Rinse were supplied by Diversey (Amsterdam, Netherlands).

4.2.2. Sample treatment

Polycarbonate samples have been preliminary washed using an ethanol-water mixture (70/30, V/V) and then rinsed with distilled water.

The best procedure for cutting pieces of the samples to submit to extraction was optimized with the aim to avoid any thermal treatment. A hollow punch having a diameter of 25 mm was used to collect samples.

An important problem in the analysis of the molecules object of this study is that these compounds are inherently ubiquitous in the laboratory environment, and they can be introduced into the sample

during sample treatment. Therefore, to preserve the sample solutions from any contamination due to possible contact with plastic material, all the laboratory procedures were performed employing glassware previously washed with distilled water and then with acetone and hexane and dried in oven at 80°C, as reported in literature (Cacho et al., 2012). All the above procedure was also extended to glass syringes and pipettes. Only PTFE filters were employed, which were previously washed with chloroform and methanol, and then emptied to remove any solvent residue.

Polycarbonate extracts were prepared following a method reported in literature (Nerin et al., 2003) and slightly modified as follows: small pieces of PC (1.5 g) were transferred to a 100 mL round flask. 12 mL of chloroform were added, and the sample was shaken with magnetic stirring to avoid adhesion of the polymer to the flask until dissolution was complete, which required about 40 min. Then, 18 mL of methanol were added with vigorous hand shaking to reprecipitate the polymer. This extract was recuperated and transferred into a clean round flask. The flask was rinsed with four additional washes with 10 mL of methanol (X2) and 20 mL of acetone (X2). The extract was evaporated by rotary evaporator and resuspended by 1 ml of methanol or acetone, and, after sonication for 4 min to remove precipitate from the flask walls, it was filtered through 0.45 and 0.22 μm PTFE filters. Blank samples were prepared in parallel, following the same procedures.

4.2.3. Analysis of the PC composition by GC-FID-IR

The analyses were carried out using GC/FID/IR. A Thermo Scientific TRACETM GC equipped with AS-3000 Autosampler with split/splitless injector and Flame Ionization Detector (FID) was used.

The separation was achieved on an Agilent Technologies capillary column (HP-5, 60m x 32 mm) with 0.50 μm film thickness. The initial oven temperature was set at 60°C and immediately ramped to 280 °C at 40 °C/min and finally increased at 10°C/min to 290°C where the temperature was held for 15 min; total run time was 21.5 min.

The gas flow rates were: air at 350 ml/min, hydrogen at 35 ml/min, and make-up gas at 30 ml/min. The carrier was helium at a flow rate of 3 ml min⁻¹.

The GC-FID and the autosampler is connected to the FT-IR spectrometer (Thermo Scientific Nicolet™ 6700) by the GC transfer line, which was maintained at 290 °C. This system is controlled by a Thermo Scientific Dionex Chromeleon chromatography software. Furthermore the OMNIC software allows to reconstruct the chromatogram through Gram-Schmidt algorithm, and to retrieve a FT-IR spectra for each point of the chromatogram.

A sample volume of 1 μL was injected and splitted in a 1:9 ratio for FID/IR detection respectively. Real-time IR spectra were obtained by collecting 4 scans, with a resolution of 8 cm⁻¹.

4.2.4. FT-IR ATR spectroscopy

IR spectra were acquired using the Nicolet iS50 FT-IR Spectrometer with Pike Smart MIRacle™ single reflection horizontal ATR (HATR) attachment containing a flat and polished diamond/ZnSe sandwich crystal of 2 mm crystal, using OMNIC software (all from Thermo Fisher, Milan, Italy). Ethanol absolute was used to clean the ATR crystal prior to the first spectral analysis of each sample. HATR-IR is a

useful way of analyzing solid samples without the need for cutting samples. Infrared spectra were taken in the spectral range from 4000 to 650 cm^{-1} .

The following samples were analysed: PC sample after photo-ageing by climatic chamber treatment (100 h, 25 °C, 50% RH, 125 W) and PC sample after rinsing with detergent and sparkling aid.

4.3. Results and discussion

4.3.1. GC-FID-IR analysis

Basing on standards analyzed in literature (Nerin et al., 2013; Gao et al., 2011), the most representative substances of the categories of plastic additives commonly used in PC were selected, as listed in Table 1. All of these standard additives were analyzed at a concentration of 50 $\mu\text{g/ml}$, singularly by GC-FID-IR; however some of them were not detected by the IR spectrometer due to their high boiling point with respect to the maximum reachable temperature by the transfer line, causing their condensation. The collected data, allowed the building a full IR data library corresponding to each standard compound. Among the standards which can be observed by the IR detector, twelve were selected, being considered particularly representative, in order to produce a mixture of compounds to be used as a reference for the analysis of the complex PC sample. The GC-FID method allowed the complete separation of the twelve standards in a retention time of about 12 minutes (Fig. 1).

Table 1. List of common additives used in PC. The asterisks indicate the ones used as standards in this work.

ANALYTE	CATEGORY	CHEMICAL CLASSIFICATION
TINUVIN 326	UV ABSORBER/LIGHT STABILIZER	BENZOTRIAZOLE
*TINUVIN 328	UV ABSORBER/LIGHT STABILIZER	BENZOTRIAZOLE
TINUVIN 327	UV ABSORBER/LIGHT STABILIZER	BENZOTRIAZOLE
TINUVIN 234	UV ABSORBER/LIGHT STABILIZER	BENZOTRIAZOLE
*CHIMASSORB 81	UV ABSORBER/LIGHT STABILIZER	BENZOPHENONE
CYASORB UV5411	UV ABSORBER/LIGHT STABILIZER	BENZOTRIAZOLE
*CYASORB UV9	UV ABSORBER/LIGHT STABILIZER	BENZOPHENONE
UVINOL 400	UV ABSORBER/LIGHT STABILIZER	BENZOPHENONE
CYASORB UV24	UV ABSORBER/LIGHT STABILIZER	BENZOPHENONE
CYASORB UV12	UV ABSORBER/LIGHT STABILIZER	BENZOPHENONE
ADVASTAB 800	ANTIOXIDANT	THIO-ESTHER
*BHA	ANTIOXIDANT	PHENOLIC
*BHT	ANTIOXIDANT	PHENOLIC
*ANTIOXIDANT YS 40	ANTIOXIDANT	PHENOLIC
*CYANOX 2246	ANTIOXIDANT	PHENOLIC
*IRGANOX 1081	ANTIOXIDANT/THERMAL STABILIZER	PHENOLIC
IRGANOX 1076	ANTIOXIDANT/THERMAL STABILIZER	PHENOLIC
IRGAFOS 168	PROCESSING STABILIZER	ARYL-PHOSPHITE
UVITEX OB	OPTICAL BRIGHTENER/WHITENING AGENT	BENZOXAZOLE
*BISPHENOL A	PC MONOMER	

BADGE	BPA DEGRADATION PRODUCT	
*9,9DIMETHYLXANTENE	BPA DEGRADATION PRODUCT	
*4 OCTYL PHENOL	BPA DEGRADATION PRODUCT	
*4 NONYL PHENOL	BPA DEGRADATION PRODUCT	

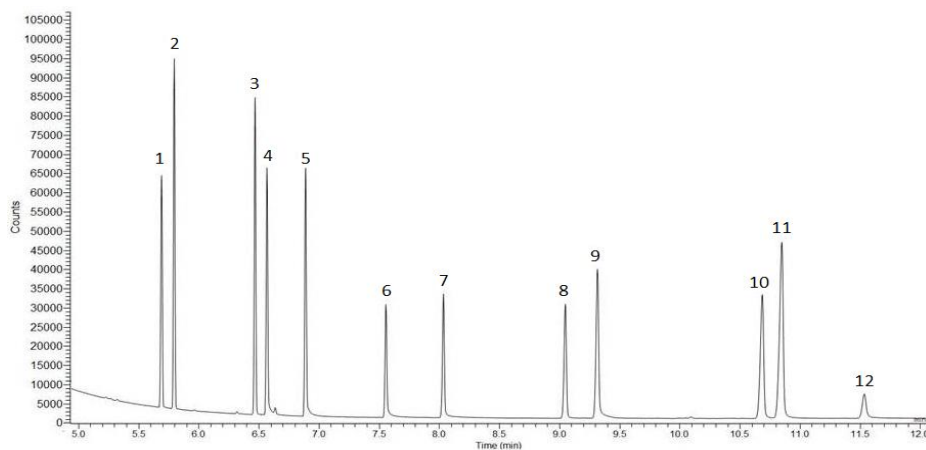


Fig. 1. GC-FID chromatogram of the standards mixture. 1: BHA; 2: BHT; 3: 9,9-DIMETILXANTENE; 4: 4-OCTYL-PHENOL; 5: 4-NONYL-PHENOL; 6: CYASORB UV9; 7: BPA; 8: CYANOX 2246; 9: IRGANOX 1081; 10: TINUVIN 328; 11: ANTYOXIDANT YS 40; 12: CHIMASSORB 81.

Similarly, the IR data were collected on the standard mixture, allowing the Gram-Schmidt reconstruction of the GC chromatogram (Figure 2).

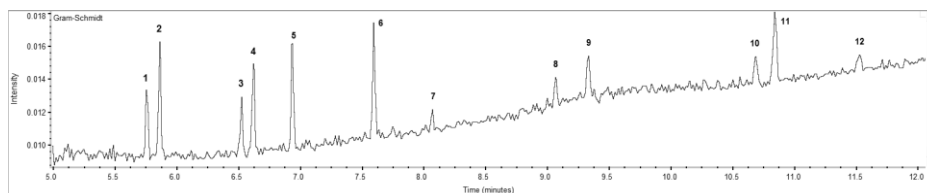


Fig. 2. Gram Schmidt of the standards mixture

The recognition of the analytes in the polycarbonate sample was done by the synergic use of GC and IR data. By comparing the retention times of the analytes in the sample (Fig. 3) with the ones of the standard mixture (Fig. 1), three peaks (marked as 2, 7 and 8 in Fig. 3) were preliminarily assigned to BHT, BPA and CYANOX 2246 respectively.

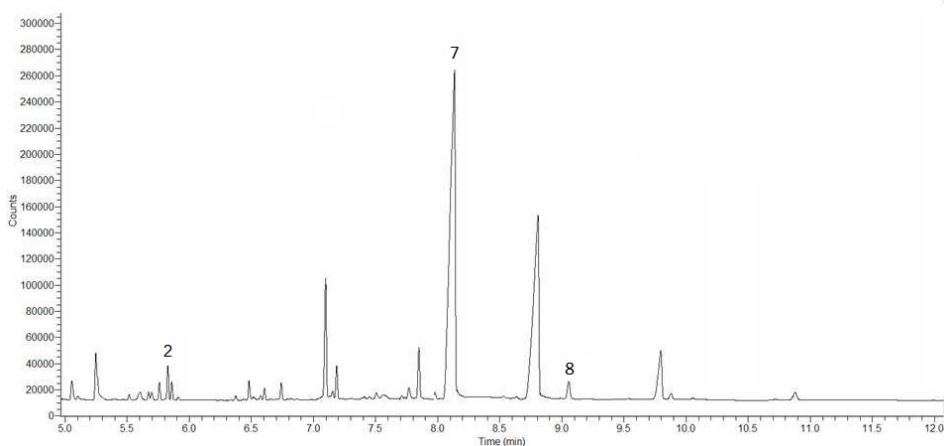


Fig. 3. GC-FID chromatogram of polycarbonate sample after dissolution. 2: BHT; 7: BPA 8: CYANOX 2246.

The IR spectra corresponding to the three peaks were compared to the ones obtained by the standards mixture, allowing to confirm the assignment carried out on the basis of the GC data.

In Figure 4 the Gram Schmidt of the polycarbonate sample, the IR spectrum corresponding to the peak 2 and the best-fitting results of the library database are reported. The data analysis confirms the previous assignment, showing an excellent qualitative match with the BHT IR spectrum. The low matching value (51.93%) is determined by the very low concentration of BHT in the sample that consequently produces

noisy data. The same procedure was performed for the analyte 7 (Fig. 5), which shows very good match (88.57%) with the standard BPA, also in this case confirming the GC data. On the other hand the analysis performed on the analyte 8 (Fig. 6) shows a low match (both by the qualitative and numerical point of view) with the library compounds, therefore not allowing an univocal assignment of the analyte identity.

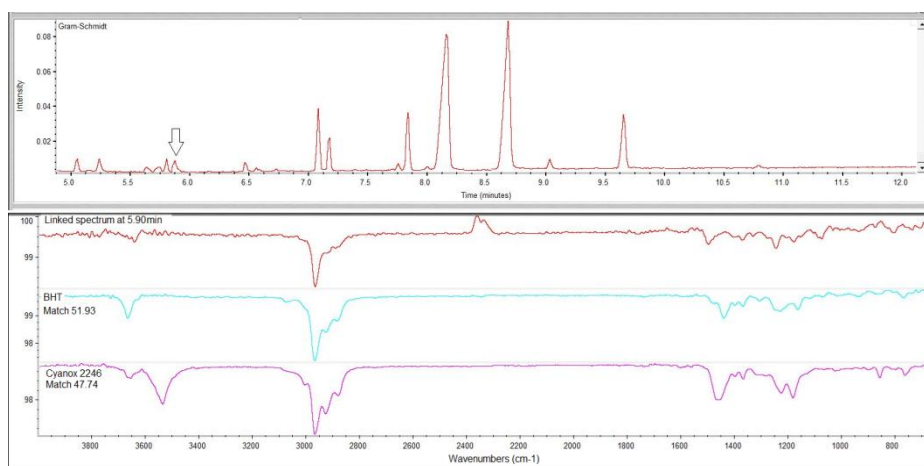
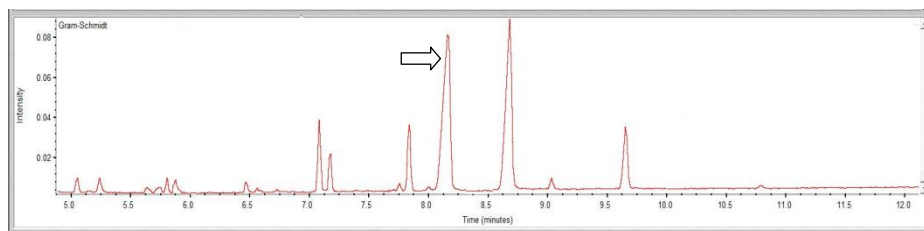


Fig. 4. Top panel: Gram Schmidt of the PC sample. Bottom panel: IR spectrum corresponding to peak 2 indicated by the arrow (red line); IR library references of BHT and Cyanox 2246 (light blue and purple lines, respectively).



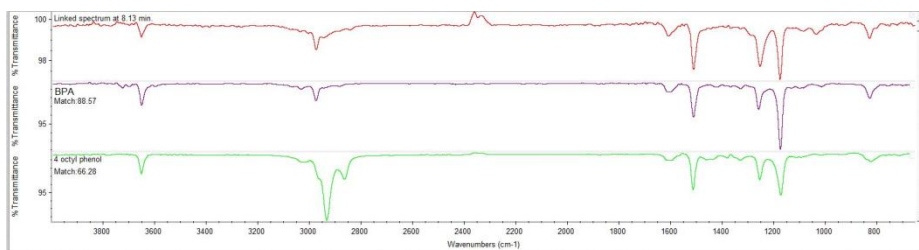


Fig. 5. Top panel: Gram Schmidt of the PC sample. Bottom panel: IR spectrum corresponding to peak 7 indicated by the arrow (red line); IR library references of BPA and 4-octyl phenol (purple and green lines, respectively).

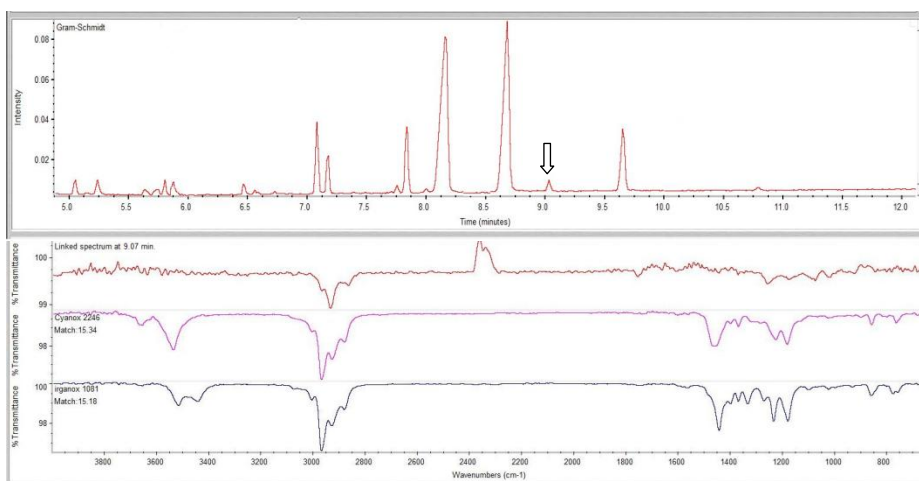


Fig. 6. Top panel: Gram Schmidt of the PC sample. Bottom panel: IR spectrum corresponding to peak 8 indicated by the arrow (red line); IR library references of Cyanox 2246 and Irganox 1081 (purple and black lines, respectively)

In order to assign the unidentified peaks, the corresponding IR spectra were analyzed. As reported in Figure 7, the IR spectra of the most relevant peaks are found to show good match with the 4-nonyl phenol and BPA standard spectrum. As a consequence we can identify these peaks as dissolution products of the PC.

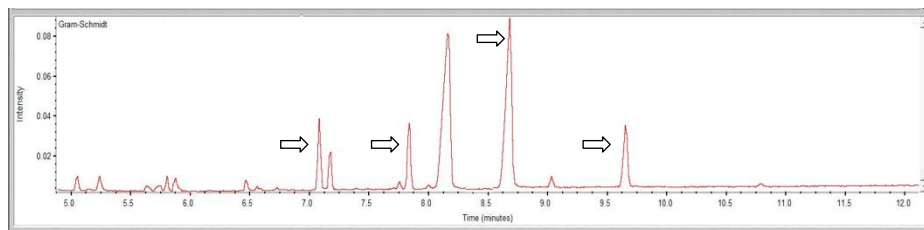


Fig. 7. Gram Schmidt of the PC sample: the arrows indicate the PC dissolution products. The best matching results obtained basing on the IR library are reported for the four peaks (left to right) in the following: uvinul 400 (match value: 19.26%); 4-nonyl-phenol (63.06%); BPA (32.22%); BPA (65.29%).

In conclusion, we can state that, as expected, most peaks occurring in the analyzed sample are constituted by PC dissolution products. Among the known additives, used as standards in our study, only BHT was identified; it cannot be excluded that some other additives were present in concentration below the sensitivity of the technique or in low purity grade. Some weak peaks remain unassigned, possibly being ascribed to unknown additives or to dissolution products.

4.3.2. FT-IR analysis in ATR mode

4.3.2.1. Photo-aging of PC

In order to verify the effects of photo-degradation of a commercial tableware, samples stored at light exposure for 100 h at 25 °C, 50% RH, 125 W in climatic chamber were examined by FT-IR in ATR mode. In Figure 10 the IR spectra of the PC before and after irradiation in climatic chamber are shown. In these conditions, the sample shows good stability, since the profiles appear almost coincident, and the absorption features characteristic of oxidation products (Lemaire et al., 1986) are not detected.

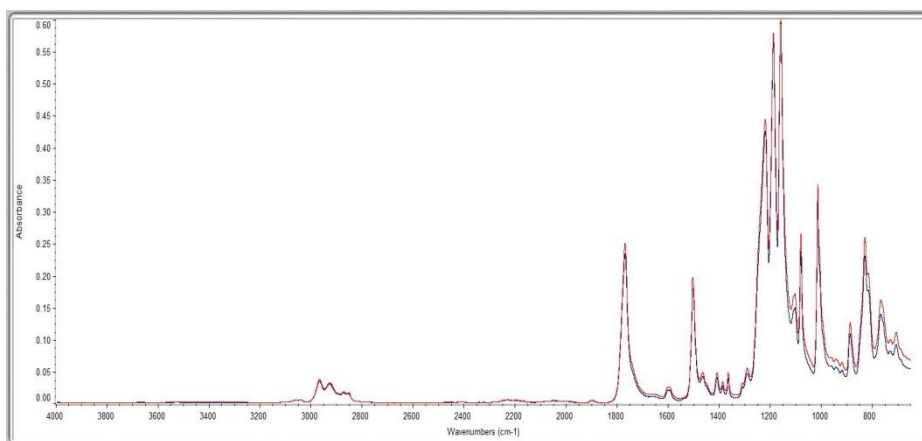


Fig. 8. IR spectra of the sample before (red) and after irradiation (blue)

4.3.2.2. Study of residues of detergent and sparkling aid

The last part of this work involved the evaluation of possible residues of detergents and sparkling aid in the tableware after common rinse operation.

In Figure 9 the IR spectra of the PC sample before and after rinse with detergent are displayed. The comparison of the two spectra shows as the only difference a broad absorption centered at about 3400 cm^{-1} corresponding to the -OH stretching in the rinsed sample, ascribed to the alkaline groups of the detergent. It is known that the residual alkaline detergent remaining on the surface of PC may increase the release of BPA (Hoekstra and Simonuau, 2013).

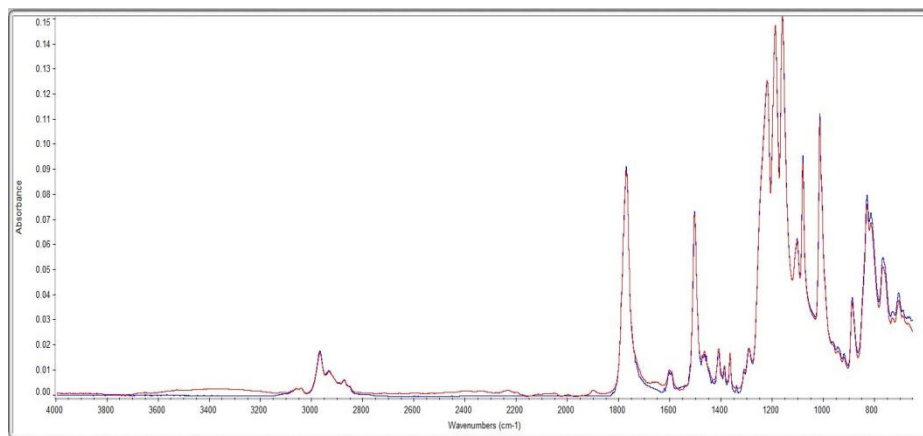


Fig. 9. IR spectra of the sample before (blue line), and after rinse with detergent (red line)

In Figure 10 the IR spectra of tableware after and before rinsing with sparkling aid are reported. The subtraction of the two spectra shows the presence of absorption features that after library search reveal excellent match with octadecane 1,2-diol, a typical component of industrial detergents.

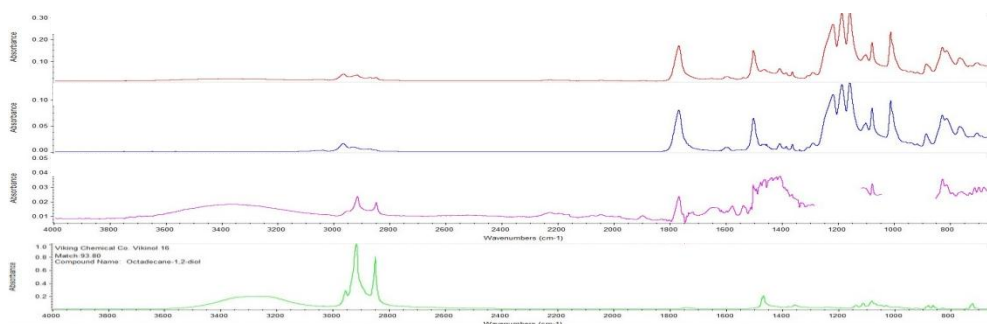


Fig. 10. IR spectra of the sample before (red line) and after (blue line) rinse with sparkling aid; subtraction of the two spectra (purple line); octadecane 1,2-diol spectra.

4.4. Conclusions

The GC-FID-FTIR system represents a new approach for the identification of potentially toxic substances occurring in food contact materials by combining GC-FID, a sensitive technique that provides information about the analytes retention time, and FTIR that provides information on the intact molecular structure resulting in a unique spectrum for each molecule. In this technique, the temperature of the transfer line is the main limit: the analytes with boiling point higher than the maximum reachable temperature by the transfer line cannot be identified. Furthermore this technique, not very sensitive, did not provide positive results for the identification of the additives that can be added in traces to PC-BPA.

The stability of the sample was tested by means of climatic chamber treatment and ATR spectroscopy. In the studied conditions the absorption features typical of oxidation products are not detected, indicating good stability of the sample.

Finally, the effects of common rinse operation with detergent and sparkling aid were studied. The obtained results indicate the presence of residuals that may increase the release of BPA; as a consequence a more accurate washing protocol should be developed in order to avoid food contaminations.

4.5. References

Alin, J., and Hakkarainen, M., 2012. Migration from polycarbonate packaging to food simulants during microwave heating. *Polymer Degradation and Stability*, 97, 1387-1395.

Arvanitoyannis, I. S., and Bosnea, L., 2004. Migration of substances from food packaging materials to foods. *Critical Reviews in Food Science and Nutrition*, 44, 63-76.

Ballesteros-Gomez, A., Rubio, S., and Perez-Bendito, D., 2009. Analytical methods for the determination of bisphenol A in food. *Journal of Chromatography A*, 1216, 449-469.

Cacho, J.I., Campillo, N., Viñas, P., and Hernández-Córdoba, M., 2012. Determination of alkylphenols and phthalate esters in vegetable and migration studies from their packages by means of stir bar sorptive extraction coupled to gas chromatography-mass spectrometry. *Journal of Chromatography A*, 1241, 21-27.

Cabado, A. G., Aldea, S., Porro, C., Ojea, G., Lago, J., Sobrado, C., and Vieites, J. M., 2008. Migration of BADGE (bisphenol A diglycidyl-ether) and BFDGE (bisphenol F diglycidyl-ether) in canned seafood. *Food and Chemical Toxicology*, 46, 1674-1680.

Cai, J., Lin, P., Zhu, X., and Su, Q., 2006. Comparative analysis of clary sage (*S. scarea* L.) oil volatiles by GC-FTIR and GC-MS. *Food chemistry*, 99, 401-407.

Collin, S., Bussière, P.O., Thérias, S., Lambert, J.M., Perdereau, J., and Gardette, J.L., 2012. Physicochemical and mechanical impacts of photo-ageing on bisphenol a polycarbonate. *Polymer Degradation and Stability*, 97, 2284-2293.

Diepens, M., and Gijsman, P., 2007. Photodegradation of bisphenol A polycarbonate. *Polymer Degradation and Stability*, 92, 397-406.

Diepens, M., and Gijsman, P., 2010. Photodegradation of bisphenol A polycarbonate with different types of stabilizers. *Polymer Degradation and Stability*, 95, 811-817.

Factor, A., and Chu, M. L., 1980. The role of oxygen in the photo-ageing of bisphenol-A polycarbonate. *Polymer Degradation and Stability*, 2, 203-223.

Factor, A., Ligon W.V., and May, R.J., 1987. The role of oxygen in the photoaging of bisphenol A polycarbonate. 2. GC/GC/high-resolution MS analysis of Florida-weathered polycarbonate. *Macromolecular*, 20, 2461-2468.

Galotto, M.J., Torres, A., Guarda, A., Moraga, N., and Romero, J., 2011. Experimental and theoretical study of LDPE versus different concentrations of Irganox 1076 and different thickness. *Food Research International*, *44*, 566–574.

Gao, Y., Gu, Y., and Wei, Y., 2011. Determination of polymer additives-antioxidants and ultraviolet (UV) absorbers by high-performance liquid chromatography coupled with UV photodiode Array detection in Food simulants. *Journal of Agricultural and Food Chemistry*, *59*(24), 12982-12989.

Hoekstra, E.J., and Simoneau, C., 2013. Release of Bisphenol A from Polycarbonate- A review. *Critical Reviews in Food Science and Nutrition*, *53*, 386-402.

Klampfl, C. W., 2013. Mass spectrometry as a useful tool for the analysis of stabilizer in polymer materials. *Trends in Analytical chemistry*, *50*, 53-64.

Lemaire, J., Gardette, J. L., Rivaton, A., and Roger, A., 1986. Dual Photochemistries in Aliphatic Polyamides, Bisphenol A Polycarbonate and Aromatic Polyurethanes-A Short Review. *Polymer Degradation and Stability*, *15*, 1-13.

Nagai, N., Okumura, H., Imai, T., and Nishiyama, I., 2003. Depth profile analysis of the photochemical degradation of polycarbonate by infrared spectroscopy. *Polymer Degradation and Stability*, *81*, 491-496.

Nerín, C., Fernández, C., Domeño, C., and Salafranca, J., 2003. Determination of Potential Migrants in Polycarbonate Containers Used for Microwave Ovens by High-Performance Liquid Chromatography with Ultraviolet and Fluorescence Detection. *Journal of Agricultural and Food Chemistry*, *51*, 5647–5653.

Oca, M.L., Ortiz, M.C., Herrero, A., and Sarabia, L.A., 2013. Optimization of GC/MS procedure that uses parallel factor analysis *Talanta*, *106*, 266–280.

Pickett, J. E., 2000. Kinetics of polycarbonate photoyellowing: an initiation/spreading model. *Polymeric Materials Science and Engineering Preprints*, *83*, 141-142.

Pickett, J. E., 2011. Influence of photo-Fries reaction products on the photodegradation of bisphenol-A polycarbonate. *Polymer Degradation and Stability*, 96, 2253-2265.

Piringer, O. G., and Baner, A. L., 2008. Characteristics of Plastic Materials. *Plastic packaging. Interactions with food and pharmaceuticals*, Chapter 2.

Reyne, M., 1991. Les Plastiques dans l'emballage. Hermès, Paris.

Zweifel H. Stabilization of polymeric materials. Berlin, Heidelberg: Springer-Verlag; 1998.

Rivaton, A., Sallert, D., and Lemaire, J., 1983. The photochemistry of bisphenol-A polycarbonate reconsidered. *Polymer Photochemistry*, 3, 463-481.

Rivaton, A., 1995 Recent advances in bisphenol A polycarbonate photodegradation. *Polymer Degradation and Stability*, 49, 163-179.

Schnoller, J., Pittenauer, E., Hutter, H., and Allmaier, G., 2009. Analysis of antioxidants in insulation cladding of copper wire: a comparison of different mass spectrometric techniques (ESI-MS, MALDI-RTOF and RTOF-SIMS). *Journal of Mass Spectrometry*, 44, 1724-1732.

Xin-Gui, L., and Mei-Rong, H., 1999. Thermal degradation of bisphenol A polycarbonate by high-resolution thermogravimetry. *Polymer International*, 48, 387-391.

SUMMARY

This PhD thesis deals with the study of different aspects of food contact materials, including active packaging and food safety controls.

In the first part of the present work the development and optimization of a simple and reproducible procedure for the realization of new antimicrobial active packaging materials is presented. The sol-gel technique was employed in order to obtain hybrid organic-inorganic films aimed at incorporating lysozyme and natamycin as active agents. The sols were properly formulated to be deposited on different substrates, and showed good adhesion and stability. In all cases the incorporation efficiency and release properties can be modulated through the modification of simple chemical and physical parameters, indicating this methodology as a good route for the realization of active packaging also on the industrial scale.

In the attempt to individuate high efficiency natural antioxidants to be employed in active packaging, the second part study of the work was focused on different steeping methods allowed to determine the best infusion conditions for extraction of antioxidants from tea leaves allowing to maximise the amount of extracted substances. Antioxidant assay and evaluation of total phenolic content were performed on the extracts indicating the tea-derived catechins as a potential active agent.

The last part of this thesis is devoted to the development of a new analytical method for the determination of potentially toxic substances released from commercial polycarbonate. The coupling of GC-FID and FTIR techniques allowed individuating some additives and most of the dissolution products of PC, as well as their degraded components, information to be used in upcoming migration analyses. Despite its low sensitivity, the technique joins the quantitative analysis features typical

of gas chromatography to the identification potentialities and chemical information of IR spectroscopy; as a result the whole technique is particularly fitting to qualitative analyses also of unknown compounds.